Low-dimensional chaos in surface waves: Theoretical analysis of an experiment

Ehud Meron and Itamar Procaccia
Department of Chemical Physics, Weizmann Institute of Science, 76100 Rehovot, Israel
(Received 20 March 1986)

A detailed theory of the appearance of low-dimensional chaos in a hydrodynamic system is presented. The system chosen has been subjected to a careful experimental study; it involves dynamics of surface waves in a cylinder of fluid which is oscillated vertically. All the major experimental findings are rationalized by the theory. It should be stressed that in addition to low-dimensional nonlinear evolution equations the theory results also in an approximate solution of the original partial differential equations.

I. INTRODUCTION

The prediction that chaos should arise as a low-dimensional phenomenon, even in systems that are described by partial differential equations (PDE's), goes back to the seminal paper of Ruelle and Takens from 1971.[1] However, the relevance of this prediction to real hydrodynamic systems was established only a decade later, after the experimental observation of Feigenbaum's period-doubling cascade[2] in a Rayleigh-Bénard system by Libchaber and Mauer.[3] Since then a growing number of experiments have appeared that prove directly (by measuring dimensions, Kolmogorov entropies, and Lyapunov exponents) that chaos sets in with low-dimensional attractors.[4] These experiments led to a renewed interest in the rather old problem of how to reduce the infinite degrees of freedom pertaining to hydrodynamic systems to the finite degrees of freedom pertaining to states at the onset of an instability.[5]

A formal theory of such a reduction exists; in principle it is based on the center-manifold theorem and on normal-form theory. A particularly compact representation of such a formal theory has been presented by Coullet and Spiegel.[6] In a subsequent study, Arneodo, Coullet, and Spiegel have applied this general framework to the rotating thermohaline system at the point of triple instability.[7] They derived nonlinear ordinary differential equations (ODE's) for the three critical degrees of freedom and showed that chaos occurs arbitrarily close to the point of instability. The rotating thermohaline system, however, is not easily accessible to experiment and therefore has not been subjected yet to experimental studies. The reason is that the salinity and temperature gradients are coupled and thus cannot be varied independently.[8] To our knowledge, in no case to date has there been a theory which describes how the reduction from the infinite to the finite occurs in practice for a hydrodynamic system on which detailed experiments have been conducted.[9] In this paper we describe a study of such a system.

The experiment we chose to analyze consists of a fluid layer in a vessel which is forced to oscillate vertically. The wave patterns which develop at the free surface of the fluid are examined. This system was studied experimentally for the first time by Faraday in 1831.[10] In that experiment Faraday found that the free surface oscillated at half the oscillation frequency of the vessel. About forty years later the problem was investigated again by Matthiessen[11] who observed a synchronous response. The discrepancy between this and Faraday's result led Lord Rayleigh[12] to make a further series of experiments which supported Faraday's view. Rayleigh also suggested[13] a theoretical approach which led to Mathieu's equation for the vertical displacement of the free surface. However, it was only in 1954 that a complete theory for the linear problem was established. The theory, proposed by Benjamin and Ursell, who have also studied the system experimentally, resolved the discrepancy in the previous observations and accounted for the various spatial modes that were observed.[14] More recently Keolian *et al.*,[15] Gollub and Meyer,[16] and Ciliberto and Gollub,[17] have repeated the experiments with the aim of studying nonlinear phenomena. It is to the experiment of Ciliberto and Gollub that we address our attention. Preliminary announcements of our theoretical results appeared in Refs. 18.

The advantage of the experiment of Ref. 17 is that there is a point in parameter space where the transition to chaos occurs essentially directly from the quiescent state. This is in contrast to all previous experiments where the chaotic motion sets in after a series of bifurcations that result in a space- and time-dependent state before the onset of chaos. In those cases the theoretical analysis called therefore for working around a complicated state.

To establish a theory for this experiment[18] we chose to adopt the method of Coullet and Spiegel.[6] This method has the advantage that the amplitude equations for the critical degrees of freedom are derived directly in normal form (see below).

The hydrodynamic equations in our example contain a time-periodic acceleration term due to the forced oscillations of the vessel. They therefore fall in the following class of PDE's (cf. Sec. III),

$$\partial_t U = M_\lambda(t)U + N[U] , \tag{1.1}$$

where $U=(U_1,U_2,\ldots,U_N)$ is a set of field variables $U_i(\mathbf{r},t)$ which are elements of $\mathscr{H}$, the space of real functions defined in a region V of the physical space, $\lambda=(\lambda_1,\lambda_2,\ldots,\lambda_P)$ is a set of P parameters, $M_\lambda(t)$ is a linear operator having 2π-periodic time dependence and

$N[U]$ is a nonlinear operator (at least quadratic). The boundary conditions may be written as

$$B_\lambda U = 0 \text{ on } \partial V , \tag{1.2}$$

where B_λ is a time-independent linear operator. The PDE's considered by Coullet and Spiegel differ from (1.1) in that they are autonomous. This difference presents no difficulties and with minor modifications we can still follow the method.

Consider now a point λ_0 in parameter space at which d spatial normal modes become marginal (in the sense that they have no exponential growth or decay in time) while all other modes remain stable (i.e., decay exponentially). We call such a point a *critical point* and its corresponding marginal modes *critical modes*. The formalism provides a method for the evaluation of an approximate solution to Eq. (1.1) for $\lambda=\lambda_0$, which has the form

$$U(\mathbf{r},t)=\sum_{i=1}^{d} \alpha_i^0[\alpha(t)]F_i(\mathbf{r})+\sum_j \beta_j[\alpha(t)]F_j(\mathbf{r}) , \tag{1.3}$$

where the amplitudes α satisfy the nonlinear ODE's or amplitude equations

$$\dot{\alpha}=J\alpha+G(\alpha) . \tag{1.4}$$

Here $F_n(\mathbf{r})$ are vector functions belonging to $\mathscr{H}^N$ (the direct product of $\mathscr{H}$ with itself N times), i and j are indices which run over the critical and stable modes, respectively, $\alpha_i^0(\alpha)$ and $\beta_j(\alpha)$ are nonlinear functions of α, α_i^0 given by

$$\alpha_i^0=\alpha_i+\nu_i(\alpha) \tag{1.5}$$

with ν_i strictly nonlinear and β_j strictly nonlinear as well, J is a diagonal matrix (or in Jordan form) having eigenvalues with zero real parts and $G(\alpha)$ is a set of strictly nonlinear functions of α.

The solution (1.3) and the amplitude equations (1.4) are derived simultaneously in a perturbative manner to the prescribed order in the amplitudes α. It is evident from Eq. (1.3) that the time dependence of the solution U is determined by that of the critical amplitudes α_i (or α_i^0). This is a manifestation of the center-manifold theorem which proves the existence of an invariant manifold $\beta_j(\alpha)$ (cf. Sec. V). The amplitudes α in turn satisfy amplitude equations (Eq. (1.4) whose nonlinear part $G(\alpha)$ has a normal form (i.e., contains the least number of nonlinear terms). This form is achieved by means of a nonlinear transformation which is applied implicitly to the original amplitudes α_i^0 and whose inverse is given by Eq. (1.5) (cf. Sec. VI).

The paper is organized as follows. In Sec. II we review the experiment. In Sec. III the PDE's describing the problem are set up. In Sec. IV we use linear analysis to identify the critical point and modes which correspond to the experimental conditions. In Sec. V we describe the center-manifold theory which allows the reduction of the PDE's to a finite system of ODE's and show its applicability to our example. Section VI describes (following Coullet and Spiegel) a general framework for implementing this reduction. Using this framework we evaluated in Sec. VII the solution U and the amplitude equations to third order in the amplitudes α. In Sec. VIII we analyze the amplitude equations numerically and compare the results with the experimental ones. Finally, in Sec. IX, we discuss some of the assumptions underlying the theory.

II. THE EXPERIMENT

The experimental set up consists basically of a plexiglass cylinder of radius $R=6.35$ cm containing water of depth $h=1$ cm which is mounted on a cone of a loudspeaker which oscillates accurately in the vertical direction. When the amplitude of the oscillations exceeds some frequency-dependent threshold value, surface wave patterns appear on the free surface of the water. The patterns were studied by refraction: an expanded parallel laser beam traverses the cell vertically and impinges on a translucent screen located above the fluid surface. The intensity field on the screen is converted to an analog signal by a vidicon camera and then digitized.

The basic modes that span the surface deformation are

$$J_l(k_{l,m}r)\times \begin{cases}\cos(l\theta)\\ \sin(l\theta)\end{cases}$$

where r is the radial coordinate, θ the azimuthal coordinate, J_l are the Bessel functions of order l, and the allowed wave numbers $k_{l,m}$ are determined by the boundary conditions. The modes can be denoted by the double index l,m. A portion of the experimental phase diagram is shown in Fig. 1. Below the parabolic stability boundaries the surface is essentially flat. Above the stability boundaries the fluid surface oscillates at half the driving frequency (i.e., the cylinder oscillation frequency) in a single stable mode. In a stroboscopic measurement synchronized at this frequency these signals appear stationary. In the shaded regions the two modes compete with each other and give rise (in the stroboscopic measurement) to slow periodic and chaotic motions. The frequency of the slow periodic motion appeared to be about 2 orders of magni-

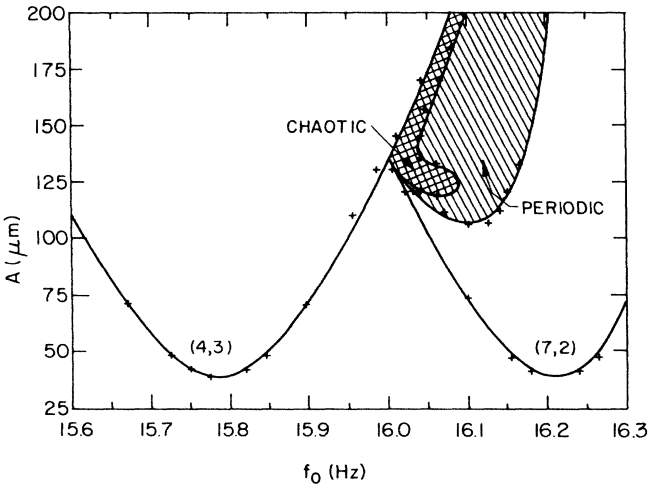

FIG. 1. Experimental phase diagram. The regions denoted (4,3) and (7,2) display stable patterns. In the shaded regions one sees slow periodic and chaotic motions.

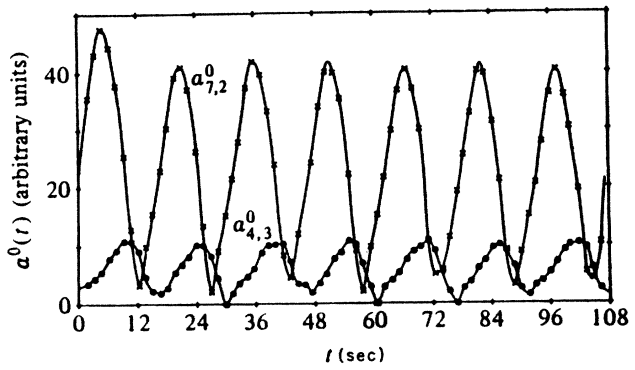

FIG. 2. Time signals (in the stroboscopic measurement) of the (4,3) and the (7,2) modes in the region of periodic competition.

tudes smaller than the driving frequency. The asymmetry in the phase diagram between the two modes suggests that the (4,3) mode damps the (7,2) mode while the latter pumps the former. Figure 2 shows time signals of both modes in the region of periodic motion. The seven-fold mode seems to lead the four-fold mode by a phase close to 90°. In the chaotic region ample evidence for the low dimensionality and the fractal structure of the attractor as well as evidence for the existence of a positive Lyapunov exponent have been found.[17]

Clearly the most interesting point in the experimental phase diagram (Fig. 1) is the point where the critical lines of the two modes meet. It appears there that the system becomes chaotic straight from the quiescent state. It thus seems worthwhile to develop the theory around this point. We shall refer to this point as the critical point and denote it by λ_0.

Ciliberto and Gollub have also studied the angular distribution of the wave patterns in the region of competition between the $l=4$ and $l=7$ modes. Figures 3 shows the angular power spectrum $P(l)$ at two different times. It is clear that in addition to the (4,3) and the (7,2) modes, many other modes with $l=1,3,4,7,8,11,14,18,21,25$, etc. are present. Given the fact that the dimension of the strange attractor found here was smaller than three, it is difficult at first sight to rationalize the active participation of so many modes. It will be seen that the theory, which provides an approximate solution of the *space- and time*-dependent surface deformation, resolves this riddle.

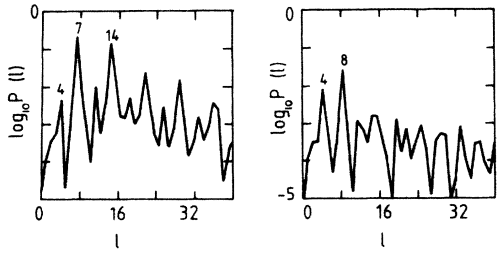

FIG. 3. Time-resolved angular power spectra showing the l modes found experimentally to be involved in the deformation pattern.

III. HYDRODYNAMICS

Consider a fluid layer of height h in a cylinder of radius R. Construct a Cartesian coordinate system which moves with the cylinder such that xy is the horizontal plane and the free surface of the fluid, in the quiescent state, is at $z=0$. For simplicity we shall neglect the viscosity of the fluid but keep in mind that viscous dissipation does exist in the system. The equation of motion for the velocity field $\mathbf{v}$ is then[14]

$$\frac{\partial \mathbf{V}}{\partial t}+(\mathbf{V}\cdot\nabla)\mathbf{V}=-\frac{1}{\rho}\nabla P+[g-\tilde{A}\cos(\omega t)]\hat{\mathbf{z}}\ , \tag{3.1}$$

where $\rho,p,g,\tilde{A}$, and ω are the density, pressure, gravitational acceleration, and the amplitude and frequency of the oscillation, respectively. Since the velocities involved are all subsonic we can assume that the fluid is incompressible

$$\nabla\cdot\mathbf{V}=0\ . \tag{3.2}$$

The advantage of neglecting the viscosity is that one can define[14] a velocity potential ϕ such that $\mathbf{V}=\nabla\phi$. Equation (3.2) can now be written as

$$\nabla^2\phi=0\ . \tag{3.3}$$

Integrating Eq. (3.1) we find[14]

$$\frac{\partial\phi}{\partial t}=\frac{1}{2}\mathbf{V}\cdot\mathbf{V}=-\frac{P}{\rho}+[g-\tilde{A}\cos(\omega t)]z\ . \tag{3.4}$$

We are interested in the motion of the free surface $z=\zeta(x,y,t)$. The pressure at the free surface is

$$P=\gamma\left[\frac{1}{R_1}+\frac{1}{R_2}\right], \tag{3.5}$$

where γ is the surface tension of the fluid and R_1 and R_2 are the principal radii of curvature at a given point of the surface. For small ζ we can estimate P as[19]

$$P=\gamma[\nabla_\perp^2\zeta-\tfrac{1}{2}\cdot(\nabla_\perp\zeta\,|\,\nabla_\perp\zeta\,|^2)]\ , \tag{3.6}$$

where $\nabla_\perp=\partial_x\hat{\mathbf{X}}+\partial_y\hat{\mathbf{Y}}$. Expanding the z-dependent terms in Eq. (3.4) around $z=0$ and then inserting Eqs. (3.6) and $z=\zeta(x,y,t)$ we obtain finally the following equation of motion correct to third order in ζ and ϕ:

$$\frac{\partial\phi}{\partial t}=[g-\tilde{A}\cos(\omega t)]\zeta-\frac{\gamma}{\rho}\nabla_\perp^2\zeta-N_2(\zeta,\phi),\quad z=0 \tag{3.7}$$

where

$$N_2(\zeta,\phi)=\tfrac{1}{2}\,|\,\nabla\phi\,|^2+\tfrac{1}{2}\zeta\frac{\partial\,|\,\nabla\phi\,|^2}{\partial z}\ . \tag{3.8}$$

In deriving Eq. (3.7) we have neglected the nonlinear surface-tension term since it is smaller than the other nonlinear terms by a factor of $\gamma/\rho h^3\omega^2\sim 10^{-3}$. We have also neglected nonlinear terms containing the time derivative ∂_t. These terms are not expected to contribute significantly to the long-time behavior of the amplitude equations.

To close Eq. (3.7) we need an equation for ζ which is

provided by the kinematic surface condition

$$\frac{D}{Dt}[\zeta(x,y,t)-z]=\frac{\partial\zeta}{\partial t}+\nabla_\perp\phi\cdot\nabla_\perp\zeta-\frac{\partial\phi}{\partial z}=0\ . \tag{3.9}$$

Again we expand around $z=0$, and use Eq. (3.3) to obtain the equation (correct to third order)

$$\frac{\partial\zeta}{\partial t}=\frac{\partial\phi}{\partial z}-N_1(\zeta,\phi),\quad z=0 \tag{3.10}$$

where

$$N_1(\zeta,\phi)=\nabla_\perp\zeta\cdot\nabla_\perp\phi+\zeta\nabla_\perp^2\phi+\frac{1}{2}\zeta^2\nabla_\perp^2\frac{\partial\phi}{\partial z}+\zeta\nabla_\perp\zeta\cdot\nabla_\perp\frac{\partial\phi}{\partial z}\ . \tag{3.11}$$

The boundary conditions for the velocity potential are

$$\frac{\partial\phi}{\partial n}=0 \tag{3.12a}$$

on the walls, and

$$\frac{\partial\phi}{\partial z}=0 \tag{3.12b}$$

at the bottom ($z=h$), where $\hat{\mathbf{n}}$ is a vector normal to the walls. For the surface deformation ζ we choose the boundary condition

$$\frac{\partial\zeta}{\partial n}=0 \tag{3.13}$$

on the walls at the free surface. This condition means that the contact angle is 90°. (For further discussion of these boundary conditions see Secs. IV and IX).

Making the transformations $(x,y,z)/h\to(x,y,z)$, $\omega t\to t$ and $\phi/\omega h^2\to\phi$ we arrive at the dimensionless equations ($z=0$)

$$\frac{\partial\zeta}{\partial t}=\frac{\partial\phi}{\partial z}-N_1(\zeta,\phi)\ , \tag{3.14a}$$

$$\frac{\partial\phi}{\partial t}=-\frac{1}{h\omega^2}\left[\frac{\gamma}{\rho h^2}\nabla_\perp^2-g+\tilde{A}\cos t\right]\zeta-N_2(\zeta,\phi)\ , \tag{3.14b}$$

where the forms of N_1 and N_2 remain unchanged. These equations have the general form of Eq. (1.1) with $U\equiv\begin{pmatrix}\zeta\\ \phi\end{pmatrix}$ and $\lambda\equiv(\tilde{A},\omega)$.

IV. LINEAR ANALYSIS

Having established the PDE's description of the system we proceed to a linear stability analysis of these equations. We shall construct a theoretical phase diagram in the vicinity of the critical point λ_0, compare it with the experimental one, and argue that no modes other than the (4,3) and (7,2) ones are expected to become marginal at λ_0.

Let us expand the solution of Eqs. (3.14),

$$U(\mathbf{r},t)=\begin{bmatrix}\zeta(x,y,t)\\ \phi(x,y,z,t)\end{bmatrix} \tag{4.1}$$

in terms of a complete orthonormal set of functions $\{f_n(x,y)\}$ belonging to $\mathscr{H}^N$, where n is a set of indices characterizing the spatial structure of f_n. Thus

$$U(\mathbf{r},t)=\sum_n\begin{bmatrix}\zeta_n(t)\\ \phi_n(t,z)\end{bmatrix}f_n(x,t)\ . \tag{4.2}$$

The functions f_n should satisfy the boundary conditions imposed on U [Eqs. (3.12) and (3.13)]. We therefore choose

$$f_{lm}=N_{lm}J_l(k_{lm}r)\cos(l\theta+\eta_l)\ , \tag{4.3}$$

where $k_{lm}r$ is the mth zero of dJ_l/dr, N_{lm} is a normalization constant, and η_l is a constant phase. Since no rotational motion has been observed in the experiment it is sufficient to include in $\{f_n\}$ only cosine terms with constant phases (see also the discussion in Sec. IV). The functions f_{lm} chosen above are eigenfunctions of $\nabla_\perp^2$,

$$\nabla_\perp^2 f_n=-(hk_n)^2 f_n\ . \tag{4.4}$$

To evaluate the z dependence of $\phi_n(t,z)$ in Eq. (4.2) we solve Eq. (3.3) with the boundary condition (3.12b) utilizing Eq. (4.4). The evaluation is presented in Appendix A. We find there that

$$\phi_n(t,z)=\phi_n(t)\frac{e^{hk_n(z-1)}+e^{-hk_n(z-1)}}{e^{hk_n}+e^{-hk_n}}\ , \tag{4.5}$$

where $\phi_n(t)\equiv\phi_n(t,z=0)$.

We now insert the expansion (4.2) into the linearized problem, set $z=0$ and take the inner product of the resulting equation with f_n. We then obtain

$$\dot{U}_n=K_{\lambda n}(t)U_n\ , \tag{4.6}$$

where

$$U_n(t)=\begin{bmatrix}\zeta_n(t)\\ \phi_n(t)\end{bmatrix}, \tag{4.7}$$

$$K_{\lambda n}(t)=\begin{bmatrix}0 & -\chi_n\\ \Gamma_n+\Lambda\cos t & 0\end{bmatrix}, \tag{4.8}$$

and where

$$\chi_n\equiv hk_n\tanh(hk_n)\ , \tag{4.9}$$

$$\Gamma_n\equiv\frac{1}{h\omega^2}\left[\frac{\gamma k_n^2}{\rho}+g\right], \tag{4.10}$$

$$\Lambda\equiv\frac{\tilde{A}}{h\omega^2}\ . \tag{4.11}$$

Equation (4.6) is a Floquet problem.[20] Let $W_{\lambda J}$ be the fundamental matrix [i.e., the matrix whose columns are the independent solutions of Eq. (4.6)]. Then, according to Floquet's theorem,

$$W_{\lambda n}=Z_{\lambda n}(t)e^{L_{\lambda n}t}\ , \tag{4.12}$$

where $Z_{\lambda n}(t)$ is a 2π-periodic matrix and $L_{\lambda n}$ is a time-independent matrix whose eigenvalues are the Floquet characteristic exponents (FCE). An important point is that by examining the real parts of the FCE's we can delineate the stability of the spatial mode n at a point λ in parameter space and thus identify critical points and modes.

The system (4.6) is equivalent to the Mathieu equation

$$\ddot{\xi}_n+\chi_n(\Gamma_n+\Lambda\cos t)\xi_n=0\ , \tag{4.13a}$$

which can also be written as

$$\ddot{\xi}_n+(\Omega_n^2+\chi_n\Lambda\cos t)\xi_n=0\ , \tag{4.13b}$$

where

$$\Omega_n\equiv\frac{\omega_n}{\omega}\equiv\frac{1}{\omega}\left[\frac{\chi_n}{h}\left[\frac{\gamma k_n^2}{\rho}+g\right]\right]^{1/2} \tag{4.14}$$

is the dimensionless natural frequency of the n mode. For the experimental conditions $\chi_n\sim O(1)$, $\Gamma_n\sim O(10^{-1})$, and $|\Lambda|\sim O(10^{-3})$. The solutions of the Mathieu equation are well known.[20,21] The stability diagram for this equation is shown in Fig. 4. The tongues correspond to mode-locked states in which the motions are either 2π or 4π periodic with an exponentially growing envelope, thus corresponding to FCE's with positive real parts. The boundaries of the tongues as well as the regions separating them correspond to FCE's with zero real parts. Upon adding a damping factor to the Mathieu equation (which may account for the viscous dissipation) the tongues are shifted upward and the regions separating them acquire FCE's with negative real parts. The boundaries still correspond to FCE's with zero real parts and thus constitute neutral stability curves.

To simplify the stability analysis of all spatial modes at the critical point it is desirable to have analytic forms for the stability curves. These are usually derived by perturbation techniques.[20] Since $|\Lambda|\ll\Gamma_n<1$ is a small parameter, perturbation methods do apply to our case. Let us derive the equations for the stability curves of the n mode $\Gamma_n=\Gamma_n(\Lambda)$, to first order in Λ. Expanding Γ_n and $U_n(t)$ in Λ,

$$\Gamma_n=\Gamma_n^{(0)}+\Lambda\Gamma_n^{(1)}+\cdots\ , \tag{4.15a}$$

$$U_n(t)=U_n^{(0)}(t)+\Lambda U_n^{(1)}(t)+\cdots\ , \tag{4.15b}$$

and inserting the expansions in Eq. (4.6) we find

$$\left[\frac{d}{dt}-K_n^{(0)}\right]U^{(0)}=0\ , \tag{4.16a}$$

$$\left[\frac{d}{dt}-K_n^{(0)}\right]U_n^{(1)}=K_n^{(1)}(t)U_n^{(0)}\ , \tag{4.16b}$$

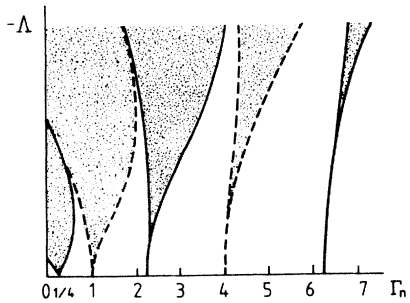

FIG. 4. Stability diagram for Mathieu's equation. The Γ_n axis is measured in units of χ_n^{-1}. The shaded tongues correspond to unstable motion. The solid and dashed lines correspond respectively to 4π- and 2π-periodic motions.

etc., where

$$K_n^{(0)}\equiv\begin{bmatrix}0 & -\chi_n\\ \Gamma_n^{(0)} & 0\end{bmatrix}\ , \tag{4.17a}$$

$$K_n^{(1)}(t)\equiv\begin{bmatrix}0 & 0\\ \Gamma_n^{(1)}+\cos t & 0\end{bmatrix}\ . \tag{4.17b}$$

The coefficients $\Gamma_n^{(0)},\Gamma_n^{(1)},\ldots$ in Eqs. (4.15a) are determined by looking for periodic solutions to Eqs. (4.16). The eigenvalues of $K_n^{(0)}$ are $\pm i(\chi_n\Gamma_n^{(0)})^{1/2}$. For $U_n^{(0)}$ to be 2π periodic we require

$$\Gamma_n^{(0)}=\frac{1}{\chi_n}(m+1)^2,\quad m=0,1,2,\ldots \tag{4.18a}$$

while to obtain 4π-periodic solutions we require

$$\Gamma_n^{(0)}=\frac{1}{\chi_n}(m+\tfrac{1}{2})^2,\quad m=0,1,2,\ldots\ . \tag{4.18b}$$

The coefficients $\Gamma_n^{(1)}$ are determined by the requirement that the right-hand side of Eq. (4.16b) should be orthogonal to the null space of the adjoint of $(d/dt-K_n^{(0)})$ where the inner product consists of integration over the period of the solutions.[22] The results are the following. When $U_n^{(1)}$ is 2π periodic,

$$\Gamma_n^{(1)}=0,\quad \text{for every } m \tag{4.19a}$$

while when $U_n^{(1)}$ is 4π periodic,

$$\Gamma_n^{(1)}=\begin{cases}\pm\frac{1}{2} & m=0\ ,\\ 0 & m>0\ .\end{cases} \tag{4.19b}$$

Thus the stability curves in the $\Lambda-\Gamma_n$ planes, to first order in Λ, are given by the following equations. For 2π-periodic solutions,

$$\Gamma_n=\frac{1}{\chi_n}(m+1)^2+O(\Lambda^2),\quad m=0,1,2,\ldots\ . \tag{4.20}$$

For 4π-periodic solutions,

$$\Gamma_n=\frac{1}{4\chi_n}\pm\tfrac{1}{2}\Lambda+O(\Lambda^2),\quad m=0 \tag{4.21a}$$

$$\Gamma_n=\frac{1}{\chi_n}(m+\tfrac{1}{2})^2+O(\Lambda^2),\quad m=1,2,\ldots\ . \tag{4.21b}$$

The boundaries of the tongues depicted in Fig. 4 can be easily identified with Eqs. (4.20) and (4.21) for $m=0,1,2$.

The stability diagrams in the Λ-Γ_n planes, each pertaining to a different spatial mode, are not of much interest for us, since it is the interaction between different spatial modes at given Λ and ω values that we want to study. What we would like to have, rather, is a single stability (or phase) diagram in the Λ-ω plane composed of critical lines of all spatial modes. This diagram is easily obtained: the map from a Γ_n axis to the ω axis is given by [see Eqs. (4.10) and (4.14)]

$$\omega=\frac{\omega_n}{\sqrt{\chi_n\Gamma_n}}\ . \tag{4.22}$$

Thus inserting Eqs. (4.20) and (4.21) in Eq. (4.22) and ex-

panding to first order in Λ we find the following critical line equations. For 2π-periodic solutions,

$$\omega=\frac{\omega_n}{m+1}+O(\Lambda^2),\quad m=0,1,2,\ldots . \tag{4.23}$$

For 4π-periodic solutions

$$\omega=2\omega_n(1\pm\chi_n\Lambda)+O(\Lambda^2),\quad m=0 \tag{4.24a}$$

$$\omega=\frac{\omega_n}{m+1/2}+O(\Lambda^2),\quad m=1,2,\ldots . \tag{4.24b}$$

Notice that the infinite series of tongues, pertinent to each spatial mode, accumulates in a finite interval $[0,2\omega_n]$ on the ω axis.

Having obtained the stability curve equations we may construct a theoretical phase diagram in any range of interest. All we must do is to look for spatial modes η, and tongues m, for which ω in Eqs. (4.23) and (4.24) falls in the prescribed range. In Fig. 5 we show the theoretical phase diagram in the range covered by the experiment. The (4,3) and (7,2) tongues are positioned fairly closely to their experimental counterparts. However, the mode (11,1), which is not seen experimentally,[23] is found between them. The reason for this is the boundary conditions chosen in Sec. III. In fact, if we pick the boundary conditions $\phi=\zeta=0$ at the walls, the (11,1) mode is pushed outside of the region of interest, and the modes (2,4) and (10,1) creep in. Our conclusion is that the experimental boundary conditions are probably neither, but a mixture of the two. We thus disregard the (11,1) mode from now on but keep in mind that the boundary conditions that we chose are not exact (cf. the discussion in Sec. IX).

Due to the absence of viscosity the stability curves start at $\Lambda=0$ and not at a finite Λ value. Thus while the ω coordinate of the critical point, estimated to be $\omega_0=\omega_{4,3}+\omega_{7,2}+O(10^{-3}\omega_0)$, is predicted fairly well, the Λ coordinate cannot be determined from the theory. We note that there are additional tongues which fall in the range of interest (i.e., $2\omega_{4,3}\lesssim\omega\lesssim 2\omega_{7,2}$), all of them being extremely narrow since their equations are not linear in Λ. Those which belong to modes having wave vectors comparable to $k_{4,3}$ or $k_{7,2}$ are sparse and bounded away from the close vicinity of the critical point. Those corresponding to modes with considerably higher wave vectors may become dense (as $n,m\to\infty$); however , due to the viscous dissipation they lie well above the critical point. It is therefore safe to conclude that only the (4,3) and (7,2) spatial modes become marginal at the critical point and that the distribution of the FCE's in the complex plane is qualitatively as shown in Fig. 6.

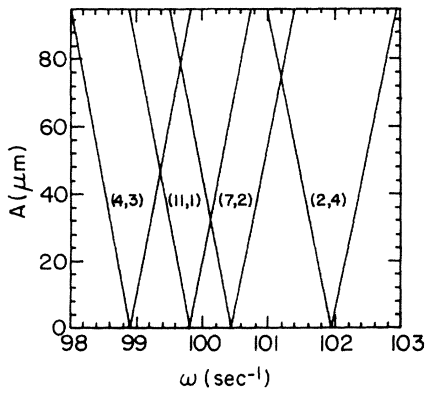

FIG. 5. Theoretical stability boundaries as predicted by the linearized theory without damping. The mode (10,1) has a tongue to the left of the mode (4,3). The ordinate is $A=2h\,|\Lambda|$.

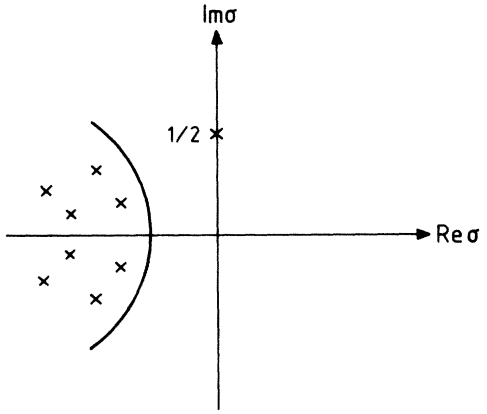

FIG. 6. Distribution of the FCE's in the complex plane.

V. APPLICATION OF CENTER-MANIFOLD THEORY

According to the linear-stability analysis of Sec. IV, when viscous dissipation is taken into account, the FCE's spectrum, for $\lambda=\lambda_0$, has the form depicted in Fig. 6. Each of the (4,3) and (7,2) modes has an FCE equal to $i/2$. All other modes have FCE's whose real parts are bounded well away from the imaginary axis. When one has such a situation in a case of *autonomous* equations of motion one can use the center-manifold theorem[24] to reduce the nonlinear dynamics to a set of ordinary differential equations. We shall firstly review this theorem and then rectify the fact that in our case we have explicit time dependence such that the theorem is of use to us as well. Let us start with the definitions of an invariant manifold and of a center manifold.

Invariant manifold. Consider the equation

$$\dot{X}=N(X)\ , \tag{5.1}$$

where $X\in R^n$. A set of $S\propto R^n$ is said to be an invariant manifold for Eq. (5.1) if for $X_0\in S$, the solution $X(t)$ of Eq. (5.1) with $X(0)=X_0$ is in S.

Consider now the system

$$\dot{X}=AX+f(X,Y)\ , \tag{5.2a}$$

$$\dot{Y}=BY+g(X,Y)\ , \tag{5.2b}$$

where $X\in R^n$, $Y\in R^m$, and A and B are constant matrices such that all the eigenvalues of A have zero real parts while all the eigenvalues of B have negative real parts. Let the functions f and g be C^2 with $f(0,0)=0$,

$Df(0,0)=0$, $g(0,0)=0$, $Dg(0,0)=0$. (Here Df is the Jacobian matrix of f).

Center manifold. An invariant manifold $y=h(x)$ for (5.2) is called a center manifold if $h:\mathbb{R}^n\to\mathbb{R}^m$ is smooth and $h(0)=0$ and $Dh(0)=0$.

The center-manifold theorem. There exists a center manifold for (5.2), $Y=h(X)$, $|X|<\delta$, where h is $\mathbb{C}^2$. The flow on the center manifold is governed by the n-dimensional system

$$\dot{S}=AS+f(S,h(S)) . \tag{5.3}$$

The significance of this theorem is that the solution $S(t)$ of Eq. (5.3) provides a good approximation for the long-time behavior of the solution $X(t)$ of Eq. (5.2). The theorem is extendable to infinite-dimensional systems ($m\to\infty$) as well.[24]

As mentioned earlier our problem is not autonomous. If we insert the expansion (4.2) into the nonlinear PDE's (3.14) and denote the amplitudes of the critical modes (4,3) and (7,2) by A_i and those of the stable modes by B_j, we obtain

$$\dot{A}_i=K_{\lambda i}(t)A_i+G_i(A,B) , \tag{5.4a}$$

$$\dot{B}_j=K_{\lambda j}(t)B_j+G_j(A,B) , \tag{5.4b}$$

where the functions G_n are strictly nonlinear in A and B. From now on we shall confine ourselves to the critical point λ_0 and omit the subscript λ from the equations. In order to apply the center-manifold theorem we make the system (5.4) autonomous with the linear part having the spectrum of Fig. 6. To obtain this form we use the transformation $Z_n(t)^{-1}$ where $Z_n(t)$ is defined by Eq. (4.12). In Appendix B we show that

$$\dot{\tilde{A}}_i=L_i\tilde{A}_i+\tilde{G}_i(\tilde{A},\tilde{B},t) , \tag{5.5a}$$

$$\dot{\tilde{B}}_j=L_j\tilde{B}_j+\tilde{G}_j(\tilde{A},\tilde{B},t) , \tag{5.5b}$$

where $\tilde{U}_n\equiv Z_n(t)^{-1}U_n$ and $\tilde{G}_n$ are strictly nonlinear functions of $\tilde{A}$ and $\tilde{B}$ having also explicit periodic time dependence. This explicit time dependence can be removed by introducing additional "critical" degrees of freedom α_c, $\bar{\alpha}_c$ defined by

$$\alpha_c=\tfrac{1}{2}\Lambda e^{it} , \tag{5.6}$$

which satisfy the "amplitude equations"

$$\dot{\alpha}_c=i\alpha_c , \tag{5.7a}$$

$$\dot{\bar{\alpha}}=-i\bar{\alpha}_c . \tag{5.7b}$$

Inserting Eq. (5.6) into the $\tilde{G}_n$'s in Eq. (5.5) we obtain an autonomous system which together with Eqs. (5.7) has the desired properties of the system (5.2). (Recall that the eigenvalues of the L_n's are the FCE's). We thus have a center manifold

$$\tilde{B}=\tilde{B}(\tilde{A}) , \tag{5.8}$$

or going back to A and B,

$$B=B(A) , \tag{5.9}$$

where A and $\tilde{A}$ in Eqs. (5.8) and (5.9) include also the critical degrees of freedom α_c and $\bar{\alpha}_c$, that is, $A=(\xi_{43},\phi_{43},\xi_{72},\phi_{72},\alpha_c,\bar{\alpha}_c)$. Inserting now $B=B(A)$ and $\Lambda\cos t=\alpha_c+\bar{\alpha}_c$ into Eq. (5.4a) we arrive at the *finite* system of amplitude equations

$$\dot{A}_i=K_iA_i+G_i(A) , \tag{5.10}$$

where K_i is a time-independent matrix given by

$$K_i=\begin{bmatrix}0 & -\chi_i\\ \Gamma_i & 0\end{bmatrix} . \tag{5.11}$$

It is convenient to diagonalize the matrices K_i. Thus introducing the complex conjugate pair $\alpha_i^0,\bar{\alpha}_i^0$,

$$\begin{bmatrix}\alpha_i^0\\ \bar{\alpha}_i^0\end{bmatrix}\equiv\frac{1}{\sqrt{2}}\begin{bmatrix}-i & \chi_i/\Omega_i\\ i & \chi_i/\Omega_i\end{bmatrix}\begin{bmatrix}\zeta_i\\ \phi_i\end{bmatrix} . \tag{5.12}$$

Equation (5.10) becomes

$$\dot{\alpha}^0=J\alpha^0+G^0(\alpha^0) \tag{5.13}$$

where $\alpha^0=(\alpha_a^0,\bar{\alpha}_a^0,\alpha_b^0,\bar{\alpha}_b^0,\alpha_c,\bar{\alpha}_c)$, and

$$J=\begin{bmatrix}i\Omega_a & 0 & 0 & 0 & 0 & 0\\ 0 & -i\Omega_a & 0 & 0 & 0 & 0\\ 0 & 0 & i\Omega_b & 0 & 0 & 0\\ 0 & 0 & 0 & -i\Omega_b & 0 & 0\\ 0 & 0 & 0 & 0 & i & 0\\ 0 & 0 & 0 & 0 & 0 & -i\end{bmatrix} . \tag{5.14}$$

Here, $a\equiv(4,3)$ and $b\equiv(7,2)$. If we define in a similar fashion the amplitudes $\beta_j^0,\bar{\beta}_j^0$ of the stable modes we may write the expansion (4.2) of $U(x,y,z=0,t)$ as

$$U=\sum_{i=a,b}\alpha_i^0(t)F_i(x,y)+\sum_{\substack{j\in\text{stable}\\ \text{modes}}}\beta_j^0[\alpha^0(t)]F_j(x,y)+\text{c.c.} , \tag{5.15}$$

where

$$F_n(x,y)=\frac{1}{\sqrt{2}}\begin{bmatrix}i\\ \Omega_n/\chi_n\end{bmatrix}f_n(x,y) . \tag{5.16}$$

We note that $G^0(\alpha^0)$ in Eq. (5.13) and $\beta^0[\alpha^0]$ in Eq. (5.15) are as yet unknown.

VI. EVALUATION OF THE NONLINEAR PART

To evaluate the nonlinear part $G^0(\alpha^0)$ of Eq. (5.13) one can choose between a number of standard methods. However, since α^0 represents six amplitudes and we want to derive G^0 to at least cubic order, there is a large number of nonlinear terms that might result. It becomes essential therefore to construct the simplest or minimal nonlinear equation. Such a construction is based on the theory of normal forms.[25] The essence of this theory is that a nonlinear transformation $\alpha^0=\alpha+v(\alpha)$ is applied to the original amplitudes α^0 so as to establish the simplest or the so-called normal form for the nonlinear part of Eq. (5.13) while leaving the linear part unchanged. The formalism

provides us with a method for the simultaneous derivation of the solution $U[x,y,\alpha(t)]$ and the amplitude equations for α *already in normal form* to a prescribed order in α. Before applying this formalism let us review a few results of normal-form theory.

A key concept in normal-form theory is that of resonance. Consider the system

$$\dot{X}=AX+f(X)\ , \tag{6.1}$$

where $X\in\mathbb{C}^n$, A has eigenvalues $\lambda=(\lambda_1,\lambda_2,\ldots,\lambda_n)$, and f is a vector-valued polynomial in X of degree $r\geq 2$ with $f(0)=Df(0)=0$.

Resonances. The n-tuple $\lambda=(\lambda_1,\lambda_2,\ldots,\lambda_n)$ of eigenvalues is said to be *resonant* if there is an n-tuple $m=(m_1,m_2,\ldots,m_n)$ of integers, $m_k\geq 0$, $\sum_k m_k\geq 2$ such that

$$\lambda_s=(m,\lambda) \tag{6.2}$$

for some $\lambda_s\in\lambda$. The relation (6.2) is called a resonance.

Poincaré Theorem. If the eigenvalues λ of (6.1) are nonresonant, there exists a formal nonlinear change of variables $x=y+h(y)$ with $h(0)=Dh(0)=0$ which reduces (6.1) to the linear system

$$\dot{Y}=AY\ . \tag{6.3}$$

Poincaré-Dulac Theorem. When the eigenvalues λ of (6.1) are resonant, there exists a formal nonlinear change of variables $x=y+h(y)$ which reduces (6.1) to the nonlinear system

$$\dot{Y}=AY+g(Y)\ , \tag{6.4}$$

where $g(y)$ contains only resonant monomials [that is, monomials $y_1^{m_1}y_2^{m_2}\cdots y_n^{m_n}$ such that $\lambda_s=(m,\lambda)$]. The system (6.4) is then said to have a normal form.

We proceed now to the derivation of the amplitude equations.[6] Let us first rewrite the PDE's (3.14) in a more convenient form. We introduce the scalar operator χ defined in terms of the spectral decomposition

$$\chi\equiv\sum_n \chi_n(\ ,f_n)f_n\ , \tag{6.5}$$

and the scalar operator

$$\Gamma\equiv-\frac{1}{h\omega^2}\left[\frac{\gamma}{\rho h^2}\nabla_\perp^2-g\right]\ . \tag{6.6}$$

In terms of these operators the PDE's (3.14) can be written as

$$\partial_t U=M(t)U+N[U]\ , \tag{6.7}$$

where

$$M(t)=\begin{bmatrix}0 & -\chi\\ \Gamma+\Lambda\cos t & 0\end{bmatrix}\ , \tag{6.8}$$

$$N_1[U]=-\nabla_\perp\zeta\cdot\nabla_\perp\phi-\zeta\nabla_\perp^2\phi+\tfrac{1}{2}\zeta^2\nabla_\perp^2\chi\phi+\zeta\nabla_\perp\zeta\cdot\nabla_\perp\chi\phi\ , \tag{6.9a}$$

$$N_2[U]=-\tfrac{1}{2}|\nabla_\perp\phi|^2-\tfrac{1}{2}(\chi\phi)^2+\zeta\nabla_\perp\phi\cdot\nabla_\perp\chi\phi-\zeta\nabla_\perp^2\phi\chi\phi \tag{6.9b}$$

and where

$$U=U(x,y,t)=\begin{bmatrix}\zeta(x,y,t)\\ \phi(x,y,z=0,t)\end{bmatrix}\ .$$

The advantage of this form is that we need not carry the z coordinate dependence of ϕ through nor set $z=0$ only after the operation of $M(t)$ and N, since now

$$\left.\frac{\partial\phi}{\partial z}\right|_{z=0}=-\chi[\phi(z=0)]\ , \tag{6.10}$$

as one can easily infer from Eqs. (4.2), (4.5), and (6.5). The operator $M(t)$ in Eq. (6.7) can be written as [cf. Eq. (5.6)]

$$M(t)=M+(\alpha_c+\bar{\alpha}_c)E\ , \tag{6.11}$$

where

$$M=\begin{bmatrix}0 & -\chi\\ \Gamma & 0\end{bmatrix} \tag{6.12}$$

and

$$E=\begin{bmatrix}0 & 0\\ 1 & 0\end{bmatrix}\ . \tag{6.13}$$

Note that

$$Mf_n=K_nf_n \tag{6.14}$$

where

$$K_n=\begin{bmatrix}0 & -\chi_n\\ \Gamma_n & 0\end{bmatrix} \tag{6.15}$$

As pointed out at the beginning of this section we want to transform the original amplitudes α^0 which satisfy Eq. (5.13) into new amplitudes α according to

$$\alpha^0=\alpha+v(\alpha)\ , \tag{6.16}$$

where $v(0)=Dv(0)=0$, such that the new amplitude equations

$$\dot{\alpha}=J\alpha+G(\alpha) \tag{5.13a}$$

have a normal form. According to the formalism which we now present, this transformation is implemented implicitly and sequentially.

The first step in this formalism is to use the fact that for sufficiently long times the motion lies essentially on a center manifold. We can therefore write

$$U(x,y,t)=V(x,y,\alpha(t))\ . \tag{6.17}$$

Taking the partial derivative of V with respect to time and using (6.16) we find

$$\partial_t V=J\alpha\cdot\partial_\alpha V+G(\alpha)\cdot\partial_\alpha V\ . \tag{6.18}$$

Combining now Eq. (6.18) with Eqs. (6.7) and (6.11) we obtain

$$\mathcal{L}V=-G(\alpha)\cdot\partial_\alpha V+(\alpha_c+\bar{\alpha}_c)EV+N[V]\ , \tag{6.19}$$

where

$$\mathcal{L}=1J\alpha\cdot\partial_\alpha-M\ . \tag{6.20}$$

Here, 1 is the unit matrix. $J\alpha\cdot\partial_\alpha$ is a scalar operator.

In order to solve Eq. (6.19) we expand the two unknowns V and G in Taylor series,

$$V=\sum_{k=1}^{\infty}V^{(k)}(x,y,\alpha)\ , \tag{6.21a}$$

$$G=\sum_{k=2}^{\infty}G^{(k)}(\alpha)\ , \tag{6.21b}$$

where $V^{(k)}$ and $G^{(k)}$ are homogeneous multinomials in α of degree k, and insert the expansions back in Eq. (6.19). A sequence of equations of the form

$$V^{(k)}=-G^{(k)}\cdot\partial_\alpha V^{(1)}+I^{(k)} \tag{6.22}$$

then results, where $I^{(k)}$ depends on lower-order quantities (i.e., on $V^{(k-1)}$, $V^{(k-2)},\ldots,V^{(1)}$ and on $G^{(k-1)}$, $G^{(k-2)},\ldots,G^{(2)}$) and therefore is known at each stage. Note that $I^{(1)}=0$ since I is formed out of nonlinear terms. $V^{(1)}$ is also known since the amplitudes of the stable modes β_j^0 are nonlinear in α^0 (or α) and to linear order $\alpha^0=\alpha$. Thus Eq. (5.15) implies

$$V^{(1)}=\sum_{i=a,b}\alpha_i(t)F_i(x,y)+\text{c.c.} \tag{6.23}$$

Equation (6.22) should be complemented by the solvability condition

$$(Z^{(k)},I^{(k)}-G^{(k)}\cdot\partial_\alpha V^{(1)})=0\ , \tag{6.24}$$

where $Z^{(k)}$ is a multinomial of degree k which belongs to the null space of the adjoint to

$$\mathcal{L}^+Z^{(k)}=0\ . \tag{6.25}$$

To find $\mathcal{L}^+$ and to impose the solvability condition we need an inner product. Therefore we should be more specific about the space on which $\mathcal{L}$ acts. Each $V^{(k)}$ is a sum of monomials in $\alpha_i,\bar{\alpha}_i$ of degree k with coefficients that may depend on spatial coordinates. The monomials are elements of P_k, the linear vector space of monomials of degree k in six variables. In that space we have the basis vectors

$$e^L=\prod_{i=a,b,c}\alpha_i^{l_i}\bar{\alpha}_i^{\bar{l}_i}\ , \tag{6.26}$$

where the $l_i,\bar{l}_i$ are integers, $L\equiv(l_a,\bar{l}_a,l_b,\bar{l}_b,l_c,\bar{l}_c)$, and

$$\sum_{i=a,b,c}(l_i+\bar{l}_i)=k\ . \tag{6.27}$$

The inner product in that space is defined by

$$(e^L,e^M)=\delta_{LM}\ . \tag{6.28}$$

The coefficients of the monomials in $V^{(k)}$ are in $\mathcal{H}^2$, the direct product of function space with itself. An element of this space may be written as $\phi=\begin{pmatrix}\phi_1\\ \phi_2\end{pmatrix}$. The inner product of two elements ϕ and $\psi\in\mathcal{H}^2$ is

$$(\phi,\psi)=\sum_{i=1}^{2}(\phi_i,\psi_i)\ , \tag{6.29}$$

where (ϕ_i,ψ_i) is an inner product in function space. Now let $P_1,P_2\in\mathcal{P}_k$ and $\phi,\psi\in\mathcal{H}^2$. Then $\phi P_1,\psi P_2$ are elements of the product space $\mathcal{P}_k\otimes\mathcal{H}^2$ with the inner product

$$(\phi P_1,\psi P_2)=(P_1,P_2)(\phi,\psi)\ . \tag{6.30}$$

Thus the operator $\mathcal{L}$ acts on $\mathcal{P}_k\otimes\mathcal{H}^2$ and the inner product in this space is given by Eq. (6.30). To solve Eq. (6.22) it will be convenient to expand $V^{(k)}$ in terms of the eigenvectors of $\mathcal{L}$ which span $\mathcal{P}_k\otimes\mathcal{H}^2$. These are given by the products $e^LF_{j:i}(i=1,2)$ where

$$F_{j:1}=\frac{1}{\sqrt{2}}\begin{bmatrix}i\\ \Omega_j/\chi_j\end{bmatrix}f_j(x,y)\ , \tag{6.31a}$$

$$F_{j:2}=\overline{F_{j:1}}\ . \tag{6.31b}$$

Note that $F_{j:i}$ defined above is equal to F_j defined by Eq. (5.16). One can easily check that

$$\mathcal{L}[e^LF_{j:1}]=(\sigma^L-i\Omega_j)e^LF_{j:k}\ , \tag{6.32a}$$

$$\mathcal{L}[e^LF_{j:2}]=(\sigma^L+i\Omega_j)e^LF_{J:2}\ , \tag{6.32b}$$

where

$$\sigma^L=JL=i\Omega_a(l_a-\bar{l}_a)+i\Omega_b(l_b-\bar{l}_b)+i(l_c-\bar{l}_c)\ . \tag{6.33}$$

[In Eq. (6.33) we considered the six-tuple L as a six-component vector.]

Let us also introduce the eigenvectors of the adjoint to M,

$$M^+=\begin{bmatrix}0&\Gamma\\ -\chi&0\end{bmatrix}\ . \tag{6.34}$$

These are given by

$$F_{j:1}^+=\frac{1}{\sqrt{2}}\begin{bmatrix}i\\ \chi_j/\Omega_j\end{bmatrix}f_j(x,y)\ , \tag{6.35a}$$

$$F_{j:2}^+=\overline{F_{j:1}^+}\ , \tag{6.35b}$$

and correspond, respectively, to the eigenvalues $-i\Omega_j$ and $i\Omega_j$. From Eqs. (6.31), (6.35), and (6.29) and from the orthonormality of the set $\{f_{lm}\}$ it follows that

$$(F_{j:i}^+,F_{j':i'})=\delta_{jj'}\delta_{ii'}\ . \tag{6.36}$$

Expanding now $V^{(k)}$ as

$$V^{(k)}=\sum_{i,j,L}P_{j:1}^Le^LF_{j:i}\ , \tag{6.37}$$

we find that

$$\mathcal{L}V^{(k)}=\sum_{j,L}\{P_{j:1}^L(\sigma^L-i\Omega_j)e^LF_{j:1}+P_{j:2}^L(\sigma^L+i\Omega_j)e^LF_{j:2}\}\ . \tag{6.38}$$

Taking the inner product of Eq. (6.38) with the vectors $e^LF_{j:i}^+$, $i=1,2$ we obtain

$$P_{j:1}^L(\sigma^L-i\Omega_j)=(I^{(k)}-G^{(k)}\cdot\partial_\alpha V^{(1)},e^LF_{j:1}^+)\ , \tag{6.39a}$$

$$P^L_{j:2}(\sigma^L+i\Omega_j)=(I^{(k)}-G^{(k)}\cdot\partial_\alpha V^{(1)},e^L F^+_{j:2})\ , \qquad (6.39b)$$

where we have used Eq. (6.22). For tuples L which correspond to nonresonant monomials, $\sigma^L\pm i\Omega_j\neq 0$, and Eqs. (6.39) can be solved for the coefficients $P^L_{j:1}$ irrespective of the form of $G^{(k)}(\alpha)$. For tuples L which do correspond to resonant monomials we must set the right-hand side of Eqs. (6.39) to zero in order to have a convergent expansion for $V^{(k)}$. Setting the right-hand side to zero, which is automatically taken care of by the solvability condition (6.24), imposes a restriction on $G^{(k)}(\alpha)$. It is this restriction which determines the coefficients of the resonant monomials in $G^{(k)}(\alpha)$.

To exploit the solvability conditions we must find the null space of $\mathscr{L}^+$, $\mathscr{N}(\mathscr{L}^+)$. To this end we expand $Z^{(k)}$ as

$$Z^{(k)}=\sum_{i,j,L} q^L_{j:i}e^L F^+_{j:i}\ , \qquad (6.40)$$

insert the expansion in Eq. (6.25) and take the inner product of the resulting equation with $e^L F_{j:i}$. We then find

$$q^L_{j:1}(\sigma^L-i\Omega_j)=0\ , \qquad (6.41a)$$

$$q^L_{j:2}(\sigma^L+i\Omega_j)=0\ . \qquad (6.41b)$$

Thus

$$z^L_{j:1}\in\mathscr{N}(\mathscr{L}^+),\quad \text{whenever } \sigma^L-i\Omega_j=0\ , \qquad (6.42a)$$

$$z^L_{j:2}\in\mathscr{N}(\mathscr{L}^+),\quad \text{whenever } \sigma^L+i\Omega_j=0\ , \qquad (6.42b)$$

where

$$z^L_{j:i}\equiv e^L F^+_{j:i}\ . \qquad (6.43)$$

We can outline now the main steps that are involved in the derivation of $G(\alpha)$ and $V(x,y,\alpha)$.

(a) We first utilize conditions (6.42) to find $(\mathscr{L}^+)$.

(b) We then use the solvability conditions $(Z^L_{j:i},I^{(k)}-G^{(k)}\cdot\partial_\alpha V^{(1)})=0$ to evaluate the coefficients of the resonant monomials in $G^{(k)}(\alpha)$.

(c) According to the Poincaré-Dulac theorem there exists a nonlinear change of variables which leaves out in $G^{(k)}(\alpha)$ only resonant monomials. We can therefore set the coefficients of all nonresonant monomials in $G^{(k)}(\alpha)$ to zero. In doing so we actually apply implicit nonlinear transformations to the amplitudes α.

(d) Once $G^{(k)}(\alpha)$ is known, Eqs. (6.39) can be used to evaluate $V^{(k)}$. The coefficients $P^L_{j:i}$ of the resonant terms remain undetermined. In most cases we can either set them equal to zero or use them to simplify the form of $G^{(k+1)}$.[6]

We illustrate this procedure in Sec. VII where we evaluate $G^{(2)}$, $V^{(2)}$, and $G^{(3)}$.

VII. THE AMPLITUDE EQUATIONS AND THE SOLUTION TO THE HYDRODYNAMIC EQUATIONS

In this section we derive the solution $V(x,y,\alpha)$ and the nonlinear part of the amplitude equations $G(\alpha)$ to second and third order in α, respectively. To avoid problems of small denominators in the expansion for $V^{(k)}$ we shall consider as resonances also relations of the form $\sigma^L\pm i\Omega_j=O(\epsilon)$ where $\epsilon\sim O(\Omega_b-\Omega_a)\ll 1$. We note that at the critical point $\Omega_a+\Omega_b=1+O(\epsilon^2)$ (cf. Sec. III).

As often occurs in problems of this kind, symmetry considerations play an important role in simplifying calculations. Let us present a symmetry argument which will be used repeatedly in the following. The argument stems from the rotational invariance of the system. The PDE's (6.7) are invariant under the transformation $r\to r$, $\theta\to\theta+\theta_0$, $V\to V$. In particular choose $\theta_0=\pi$. Then from Eq. (4.3), $f_{43}\to f_{43}$ and $f_{72}\to -f_{72}$ under the transformation. For $V^{(1)}$ [Eq. (6.23)] to be invariant we require that

$$\alpha_{43}\to\alpha_{43}\ ,$$
$$\alpha_{72}\to-\alpha_{72}\ , \qquad (7.1)$$

when the transformation is made. This can occur if the amplitude equation (6.16) is invariant under the transformation (7.1). As we shall see below the requirement for this invariance will save a considerable amount of calculation.

The terms of the linear order $k=1$ are already known: $G^{(1)}(\alpha)=0$, and $V^{(1)}(\alpha)$ is given by

$$V^{(1)}=\alpha_a F_{a:1}+\alpha_b F_{b:1}+\bar\alpha_a F_{a:2}+\bar\alpha_b F_{b:2}\ . \qquad (6.23')$$

We now turn to higher orders.

A. $k=2$

We start with the identification of $\mathscr{N}(\mathscr{L}^+|_{k=2})$. using (6.42) and (6.33) we find that

$$\mathscr{N}(\mathscr{L}^+|_{k=2})=\text{span}\{z^{1_{\bar n}1_c}_{n:1},z^{1_m1_{\bar c}}_{n:2}\,|\,n,m=a,b\}\ ,$$

where we have adopted the notation

$$L=(l_a,\bar l_a,l_b,\bar l_b,l_c,\bar l_c)$$
$$\equiv(l_a)_a(\bar l_a)_a(l_b)_b(\bar l_b)_{\bar b}(l_c)_c(\bar l_c)_{\bar c}\ ,$$

and where zero powers are ignored. Thus, for example, $L=1_a1_{\bar c}$ stands for $L=(1,0,0,0,0,1)$, $L=2_{\bar b}1_c$ stands for $L=(0,0,0,2,1,0)$, etc.

To exploit the solvability conditions we first evaluate the quantity $G^{(2)}\cdot\partial_\alpha V^{(1)}$. Using Eq. (6.23') for $V^{(1)}$ we immediately find

$$G^{(2)}\cdot\partial_\alpha V^{(1)}=(G^{(2)}_a F_{a:1}+G^{(2)}_b F_{b:1})+\text{c.c.} \qquad (7.2)$$

Here $G^{(2)}_a$ and $G^{(2)}_b$ represent, respectively, the quadratic part of the amplitude equations for α_a and α_b. The resonant monomials in $G^{(2)}(\alpha)$ are obtained by inserting Eq. (7.2) into the solvability conditions. The solvability condition $(z^{1_{\bar a}1_c}_{a:1},\ I^{(2)}-G^{(2)}\cdot\partial_\alpha V^{(1)})=0$, for example, yields $(G^{(2)}_a,\bar\alpha_a\alpha_c)=(I^{(2)},\bar\alpha_a\alpha_c F^+_{a:1})$ and thus $G^{(2)}_a$ should contain the term $(I^{(2)},\bar\alpha_a\alpha_c F^+_{a:1})\bar\alpha_a\alpha_c$. We need not evaluate $G^{(2)}_{\bar a}$ and $G^{(2)}_{\bar b}$ (the quadratic parts in the amplitude equations for $\bar\alpha_a$ and $\bar\alpha_b$) since these are complex conjugate to $G^{(2)}_a$ and $G^{(2)}_b$, respectively. The results for $G^{(2)}_a$ and $G^{(2)}_b$ are as follows:

$$G^{(2)}_a=(I^{(2)},\bar\alpha_a\alpha_c F^+_{a:1})\bar\alpha_a\alpha_c$$
$$+(I^{(2)},\bar\alpha_b\alpha_c F^+_{a:1})\bar\alpha_b\alpha_c\ , \qquad (7.3a)$$

$$G_b^{(2)}=(I^{(2)},\bar{\alpha}_b\alpha_c F_{b:1}^+)\bar{\alpha}_b\alpha_c + (I^{(2)},\bar{\alpha}_a\alpha_c F_{b:1}^+)\bar{\alpha}_a\alpha_c \ . \tag{7.3b}$$

By the angular-symmetry argument presented at the beginning of the section, the coefficients of the last terms in Eqs. (7.3) should vanish (the amplitude equations should be invariant under the transformation $\alpha_a\rightarrow\alpha_a,\alpha_b\rightarrow-\alpha_b$). In Appendix C we evaluate $I^{(k)}$. For $k=2$ we find

$$I^{(2)}=(\alpha_c+\bar{\alpha}_c)\begin{bmatrix}0&0\\1&0\end{bmatrix}V^{(1)}+N[V^{(1)}V^{(1)}] \ . \tag{7.4}$$

The term $N[V^{(1)}V^{(1)}]$ will not contribute to the coefficients in Eqs. (7.3) since it does not contain monomials whch involve α_c. Substituting Eq. (7.4) in Eqs. (7.3) we find

$$G_a^{(2)}=-\frac{i\chi_a}{2\Omega_a}\bar{\alpha}_a\alpha_c \ , \tag{7.5a}$$

$$G_b^{(2)}=-\frac{i\chi_b}{2\Omega_b}\bar{\alpha}_b\alpha_c \ . \tag{7.5b}$$

We turn now to the derivation of $V^{(2)}$. We shall see that the expansion

$$V^{(2)}=\sum_{i,j,L}P_{j:1}^L e^L F_{j:i} \tag{6.37'}$$

contains not only the critical modes (4,3) and (7,2) but also spatial modes (l,m), with $l=0,3,8,11,14$. The appearance of these stable modes corroborates the experimental angular power spectrum shown in Fig. 3.

We consider first monomials which contain α_c or $\bar{\alpha}_c$. Since $V^{(2)}$ should be invariant under the transformation $r\rightarrow r$, $\theta\rightarrow\theta+\pi$ we cannot associate the monomials $\alpha_a\alpha_c$, $\bar{\alpha}_a\alpha_c$, $\alpha_a\bar{\alpha}_c$, $\bar{\alpha}_a\bar{\alpha}_c$, with $F_{b:i}$ nor the monomials $\alpha_b\alpha_c$, $\bar{\alpha}_b\alpha_c$, $\alpha_b\bar{\alpha}_c$, $\bar{\alpha}_b\bar{\alpha}_c$ with $F_{a:i}$. The coefficients of these terms should therefore vanish. Moreover, for stable modes Eqs. (6.39) imply

$$P_{j:1}^L=\frac{1}{\sigma^L-i\Omega_j}(N[V^{(1)}V^{(1)}],e^L F_{j:1}^+) \ , \tag{7.6a}$$

$$P_{j:2}^L=\frac{1}{\sigma^L+i\Omega_j}(N[V^{(1)}V^{(1)}],e^L F_{j:2}^+) \ , \tag{7.6b}$$

where use has been made of Eq. (7.4) and of the orthogonality of the functions f_{lm}. Since $N[V^{(1)}V^{(1)}]$ does not contain monomials which involve α_c or $\bar{\alpha}_c$ all coefficients $P_{j:i}^L$ for stable modes and for monomials L which involve α_c or $\bar{\alpha}_c$ should vanish. The remaining terms (involving either α_c or $\bar{\alpha}_c$) are evaluated according to Eqs. (6.39). The results are the following:

$$P_{n:1}^{1_n 1_{\bar{c}}}=-\frac{\chi_n}{2\Omega_n} \ , \tag{7.7a}$$

$$P_{n:1}^{1_n 1_c}=\frac{\chi_n}{2\Omega_n} \ , \tag{7.7b}$$

$$P_{n:1}^{1_{\bar{n}} 1_{\bar{c}}}=\frac{1}{1+2\Omega_n}\frac{\chi_n}{2\Omega_n} \ , \tag{7.7c}$$

$$P_{n:1}^{1_{\bar{n}} 1_c}=0 \ , \tag{7.7d}$$

where n is either a or b. The coefficients $P_{n:2}^{1_{\bar{n}} 1_c}$, $P_{n:2}^{1_{\bar{n}} 1_{\bar{c}}}$, $P_{n:2}^{1_n 1_n}$, and $P_{n:2}^{1_n 1_{\bar{c}}}$ are the complex conjugate of those displayed above, respectively. The coefficients of monomials which involve both α_c and $\bar{\alpha}_c$ vanish since $I^{(2)}-G^{(2)}\cdot\partial_\alpha V^{(1)}$ does not contain such monomials.

We consider monomials which involve two of the four amplitudes $\alpha_a,\bar{\alpha}_a,\alpha_b,\bar{\alpha}_b$. For these monomials Eqs. (6.39) together with Eqs. (7.2), (7.5), and (7.4) imply

$$P_{j:1}^L=\frac{1}{\sigma^L-i\Omega_j}(N[V^{(1)}V^{(1)}],e^L F_{j:1}^+) \ , \tag{7.8a}$$

$$P_{j:2}^L=\frac{1}{\sigma^L+i\Omega_j}(N[V^{(1)}V^{(1)}],e^L F_{j:2}^+) \ . \tag{7.8b}$$

According to Appendix C and Eq. (6.23'), the spatial part of $N[V^{(1)}V^{(1)}]$ contains the combinations $\nabla_\perp f_i\cdot\nabla_\perp f_j$ and $f_i f_j$ where i and j represent critical modes. According to Eq. (4.3) the inner products $(f_{l_1,m_1}f_{l_2,m_2},f_{l,m})$ and $(\nabla_\perp f_{l_1,m_1}\cdot\nabla_\perp f_{l_2,m_2},f_{l,m})$ do not vanish only when

$$l=l_1+l_2 \tag{7.9a}$$

or

$$l=|l_1-l_2| \ . \tag{7.9b}$$

None of these conditions is satisfied when all the three indices l,l_1, and l_2 represent critical modes. We therefore conclude that both $P_{a:1}^L$ and $P_{b:i}^L$ vanish for the monomials L under consideration. We also conclude that among the stable modes, only those for which $l=0,3,8,11,14$ show up. [Only these l values satisfy the conditions (7.9) when l_1 and l_2 represent the critical modes 4 and 7.] The coefficients corresponding to these spatial modes are derived by straightforward calculations according to Eqs. (7.8). The results are the following:

$$P_{j:1}^{2_n}=\frac{i\Omega_n}{2\sqrt{2}\chi_n(2\Omega_n-\Omega_j)}\left[H_{nnj}+\frac{\Omega_n\chi_j}{2\Omega_j\chi_n}I_{nnj}\right] \ , \tag{7.10a}$$

$$P_{j:1}^{2_{\bar{n}}}=\frac{i\Omega_n}{2\sqrt{2}\chi_n(2\Omega_n+\Omega_j)}\left[H_{nnj}-\frac{\Omega_n\chi_j}{2\Omega_j\chi_n}I_{nnj}\right] \ , \tag{7.10b}$$

$$P_{j:1}^{1_n 1_{\bar{n}}}=-\frac{i\chi_j\Omega_n^2}{2\sqrt{2}\chi_n^2\Omega_j^2}I_{nnj} \ , \tag{7.10c}$$

where n is either a or b and $j\in\{(l,m)\,|\,l=0.8$ if $n=a$ and $l=0,14$ if $n=b\}$,

$$P_{j:1}^{1_a 1_b}=\frac{i}{2\sqrt{2}(\Omega_a+\Omega_b-\Omega_j)}\left[\left[\frac{\Omega_a}{\chi_a}+\frac{\Omega_b}{\chi_b}\right]J_{abj}-h^2\left[\frac{\Omega_a}{\chi_a}k_a^2+\frac{\Omega_b}{\chi_b}k_b^2\right]K_{abj}+\frac{\Omega_a\Omega_b\chi_j}{\chi_a\chi_b\Omega_j}I_{abj}\right] \ , \tag{7.10d}$$

$$P_{j:1}^{1_{\bar{a}} 1_{\bar{b}}}=\frac{i}{2\sqrt{2}(\Omega_a+\Omega_b+\Omega_j)}\left[\left[\frac{\Omega_a}{\chi_a}+\frac{\Omega_b}{\chi_b}\right]J_{abj}-h^2\left[\frac{\Omega_a}{\chi_a}k_a^2+\frac{\Omega_b}{\chi_b}k_b^2\right]K_{abj}-\frac{\Omega_a\Omega_b\chi_j}{\chi_a\chi_b\Omega_j}I_{abj}\right] \ , \tag{7.10e}$$

$$P_{j:1}^{1_{\bar a}1_b}=\frac{i}{2\sqrt{2}(\Omega_b-\Omega_a-\Omega_j)}\left[\left[\frac{\Omega_a}{\chi_a}-\frac{\Omega_b}{\chi_b}\right]J_{abj}-h^2\left[\frac{\Omega_a}{\chi_a}k_a^2-\frac{\Omega_b}{\chi_b}k_b^2\right]K_{abj}+\frac{\Omega_a\Omega_b\chi_j}{\chi_a\chi_b\Omega_j}I_{abj}\right], \tag{7.10f}$$

$$P_{j:1}^{1_a1_{\bar b}}=\frac{i}{2\sqrt{2}(\Omega_b-\Omega_a+\Omega_j)}\left[\left[\frac{\Omega_a}{\chi_a}-\frac{\Omega_b}{\chi_b}\right]J_{abj}-h^2\left[\frac{\Omega_a}{\chi_a}k_a^2-\frac{\Omega_b}{\chi_b}k_b^2\right]K_{abj}-\frac{\Omega_a\Omega_b\chi_j}{\chi_a\chi_b\Omega_j}I_{abj}\right], \tag{7.10g}$$

where $j\in\{(l,m)\mid l=3,11\}$. Here,

$$K_{nmj}=(f_nf_m,f_j)\,, \tag{7.11a}$$

$$J_{nmj}=(\nabla_\perp f_n\cdot\nabla_\perp f_m,f_j)\,, \tag{7.11b}$$

$$J_{nmj}=J_{nmj}+\chi_n\chi_mK_{nmj}\,, \tag{7.11c}$$

$$H_{nmj}=J_{nmj}-h^2k_n^2K_{nmj}\,. \tag{7.11d}$$

The coefficients $P_{j:2}^{2_{\bar n}}$, $P_{j:2}^{2_n}$, $P_{j:2}^{1_n1_{\bar n}}$, $P_{j:2}^{1_{\bar a}1_{\bar b}}$, $P_{j:2}^{1_a1_b}$, $P_{j:2}^{1_a1_{\bar b}}$, and $P_{j:2}^{1_{\bar a}1_b}$ are the complex conjugate of those displayed above, respectively.

We may write now on the final form for $V^{(2)}$,

$$V^{(2)}=\sum_{n=a,b}v_{n:1}^{(2)}F_{n:1}+\sum_{j\in S_2}v_{j:1}^{(2)}F_{j:1}\,, \tag{7.12}$$

where

$$v_{n:1}^{(2)}=\frac{\chi_n}{2\Omega_n}\left[\alpha_n\alpha_c-\alpha_n\bar\alpha_c+\frac{1}{1+2\Omega_n}\bar\alpha_n\bar\alpha_c\right], \tag{7.13a}$$

$$\begin{aligned}v_{j:1}^{(2)}=\sum_{n=a,b}&(P_{j:1}^{2_n}\alpha_n^2+P_{j:1}^{2_{\bar n}}\bar\alpha_n^2+P_{j:1}^{1_n1_{\bar n}}\alpha_n\bar\alpha_n\\&+P_{j:1}^{1_a1_b}\alpha_a\alpha_b+P_{j:1}^{1_{\bar a}1_b}\bar\alpha_a\alpha_b\\&+P_{j:1}^{1_a1_{\bar b}}\alpha_a\bar\alpha_b+P_{j:1}^{1_{\bar a}1_{\bar b}}\bar\alpha_a\bar\alpha_b)\,,\end{aligned} \tag{7.13b}$$

and $S_2=\{(l,m)\mid l=0,3,8,11,14\}$ (with this notation some of the coefficients $P_{j:1}^L$ are zero, for example, $P_{8,m:1}^{ab}=0$).

B. $k=3$

As before we start with the identification of $\mathcal{N}(\mathcal{L}^+\mid_{k:3})$. Using (6.43) and (6.33) we find that

$$\mathcal{N}(\mathcal{L}^+\mid_{k=3})=\text{span}\{z_{n:1}^{1_m1_l1_k},z_{n:1}^{1_m1_c1_{\bar c}},z_{n:2}^{1_{\bar m}1_l1_k},z_{n:2}^{1_{\bar m}1_c1_{\bar c}}\mid n,m,l,k=a,b\}'\,,$$

where the prime denotes that each vector $z_{n:i}^L$ appears only once [$\mathcal{N}(\mathcal{L}^+\mid_{k=3})$ is spanned by 32 independent vectors]. Proceeding in exactly the same way as for the case $k=2$ we find

$$G_n^{(3)}=\sum_{m=a,b}\left[(I^{(3)},z_{n:1}^{1_m1_c1_{\bar c}})\alpha_m\mid\alpha_c\mid^2+\sum_{l,k=a,b}{}'(I^{(3)},z_{n:k}^{1_m1_l1_{\bar k}})\alpha_m\alpha_l\bar\alpha_k\right], \tag{7.14}$$

where $n=a,b$ and the prime denotes that each monomial is counted only once. Equation (7.14) contains eight terms of which four are forbidden by symmetry. For $n=a$ these four terms are $\alpha_a^2\bar\alpha_b$, $\mid\alpha_b\mid^2\alpha_b$, $\mid\alpha_a\mid^2\alpha_b$, and $\alpha_b\mid\alpha_c\mid^2$. Every term in the amplitude equation for α_a should be invariant under the transformation (7.1). The monomials displayed above fail to satisfy this requirement. Among the four terms left in Eq. (7.14) the term $\alpha_n\mid\alpha_c\mid^2$ can be ignored since $\mid\alpha_c\mid^2=\Lambda^2/4\ll\Omega_n$. The form of $G_a^{(3)}$ is therefore given by

$$G_a^{(3)}=g_{a1}^{(3)}\mid\alpha_a\mid^2\alpha_a+g_{a2}^{(3)}\mid\alpha_b\mid^2\alpha_a+g_{a3}^{(3)}\alpha_b^2\bar\alpha_a\,, \tag{7.15}$$

where

$$g_{a1}^{(3)}=(I^{(3)},\mid\alpha_a\mid^2\alpha_aF_{a:1}^+)\,, \tag{7.16a}$$

$$g_{a2}^{(3)}=(I^{(3)},\mid\alpha_b\mid^2\alpha_aF_{a:1}^+)\,, \tag{7.16b}$$

$$g_{a3}^{(3)}=(I^{(3)},\alpha_b^2\bar\alpha_aF_{a:1}^+)\,. \tag{7.16c}$$

The form of $G_b^{(3)}$ is symmetric to that of $G_a^{(3)}$ where a and b are interchanged everywhere.

The evaluation of the coefficients $g_{ai}^{(3)}$ in Eqs. (7.16) is straightforward but involves tedious algebra. We report here only the results,

$$g_{a1}^{(3)}=\frac{1}{2\sqrt{2}}\sum_{j\in S_2}\left[\left[\frac{\Omega_j}{\chi_j}v_j^{2_a}-\frac{\Omega_a}{\chi_a}\eta_j^{1_a1_{\bar a}}-\frac{\Omega_a}{\chi_a}\eta_j^{2_a}\right]H_{aja}-\frac{\Omega_j}{\chi_j}v_j^{2_a}I_{aja}\right]+S_{aa}\,, \tag{7.17a}$$

$$\begin{aligned}g_{a2}^{(3)}=\frac{1}{2\sqrt{2}}\sum_{j\in S_2}\Bigg[&\left[\frac{\Omega_j}{\chi_j}\nu_j^{1_a1_b}+\frac{\Omega_j}{\chi_j}\nu_j^{1_{\bar a}1_b}-\frac{\Omega_b}{\chi_b}\eta_j^{1_a1_b}-\frac{\Omega_b}{\chi_b}\eta_j^{1_{\bar a}1_b}\right]H_{bja}-\frac{\Omega_a}{\chi_a}\eta_j^{1_b1_{\bar b}}H_{aja}\\&+\frac{\Omega_j}{\chi_j}(\nu_j^{1_{\bar a}1_b}-\nu_j^{1_a1_b})I_{bja}\Bigg]+2S_{ab}-R_{ab}\,,\end{aligned} \tag{7.17b}$$

$$g_{a3}^{(3)}=\frac{1}{2\sqrt{2}}\sum_{j\in S_2}\left[\left[\frac{\Omega_j}{\chi_j}\nu_j^{2_b}-\frac{\Omega_a}{\chi_a}\eta_j^{2_b}\right]H_{aja}-\left[\frac{\Omega_j}{\chi_j}\nu_j^{1_{\bar{a}}1_b}+\frac{\Omega_b}{\chi_b}\eta_j^{1_{\bar{a}}1_b}\right]H_{bja}-\frac{\Omega_j}{\chi_j}\nu_j^{2_b}I_{aja}-\frac{\Omega_j}{\chi_j}\nu_j^{1_{\bar{a}}1_b}I_{bja}\right]+S_{ab}+R_{ab}\ , \tag{7.17c}$$

where

$$\nu_j^{1_l1_m}=P_{j:1}^{1_l1_m}+P_{j:2}^{1_l1_m}\ , \tag{7.18a}$$

$$\eta_j^{1_l1_m}=P_{j:1}^{1_l1_m}-P_{j:2}^{1_l1_m}\ , \tag{7.18b}$$

$$S_{ab}=\frac{ih^2}{8}(\Omega_a k_a^2+2\Omega_b k_b^2)(f_a f_b^2,f_a)\ , \tag{7.19a}$$

$$S_{aa}=\frac{3ih^2}{8}\Omega_a k_a^2(f_a^3,f_a)\ , \tag{7.19b}$$

$$R_{ab}=\frac{i\Omega_a}{2}(\nabla_\perp f_a\cdot\nabla_\perp f_b f_b,f_a)-\frac{i\Omega_b}{2}(|\nabla_\perp f_b|^2 f_a,f_a)\ . \tag{7.19c}$$

We shall not evaluate $V^{(3)}$ here but only note that in addition to the critical modes it contains new stable modes $j\in S_3$, where $S_3=\{(l,m)\,|\,l=1,10,12,15,18,21\}$.

To summarize this section let us combine the results obtained for $G^{(k)}$ and $V^{(k)}$ and write the final forms for the amplitude equations and for the solution $V(x,y,\alpha)$. The amplitude equations read

$$\dot{\alpha}_a=i\Omega_a\alpha_a+i\gamma_1 e^{it}\bar{\alpha}_a+i\gamma_2|\alpha_a|^2\alpha_a+i\gamma_3|\alpha_b|^2\alpha_a+i\gamma_4\alpha_b^2\bar{\alpha}_a\ , \tag{7.20a}$$

$$\dot{\alpha}_b=i\Omega_b\alpha_b+i\delta_1 e^{it}\bar{\alpha}_b+i\delta_2|\alpha_b|^2\alpha_b+i\delta_3|\alpha_a|^2\alpha_b+i\delta_4\alpha_a^2\bar{\alpha}_b\ , \tag{7.20b}$$

where γ_i and δ_i are real and given by

$$\gamma_1=-\frac{\chi_a\Lambda}{4\Omega_a},\quad \delta_1=-\frac{\chi_b\Lambda}{4\Omega_b}\ , \tag{7.21a}$$

$$\gamma_{j+1}=-ig_{aj}^{(3)},\quad \delta_{j+1}=-ig_{bj}^{(3)},\quad j=1,2,3\ . \tag{7.21b}$$

The space- and time-dependent solution reads

$$V=\left[\sum_{i=a,b}[\alpha_i+v_i^{(2)}(\alpha)+v_i^{(3)}(\alpha)]F_i(x,y)+\sum_{j\in S_2}v_j^{(2)}(\alpha)F_j(x,y)+\sum_{j\in S_3}v_j^{(3)}(\alpha)F_j(x,y)\right]+\text{c.c.}\ , \tag{7.22}$$

where $v_i^{(2)}$ and $v_j^{(2)}$ are given by Eqs. (7.13a) and (7.13b), respectively, and $F_i\equiv F_{i:1}$. Note that Eq. (7.22) has the form of Eq. (1.3).

VIII. NUMERICAL RESULTS AND COMPARISON WITH THE EXPERIMENT

The analytic expressions obtained for the coefficients γ_i,δ_i in the amplitude equations can be used, in principle, to calculate the coefficients theoretically for the specific experimental conditions. However, several difficulties, pertaining to the basis functions $f_{l,m}$ [Eq. (4.3)], arise when we embark on such a calculation. The first difficulty is related to the inexact boundary condition $\partial\zeta/\partial n=0$ which results in an inaccurate set of basis functions. The unknown constant phases η_l present another difficulty. Thirdly, the absence of orthogonality relations for the integrals (7.11a) and (7.11b) with respect to the radial index m calls for an evaluation of a large number of integrals. Thus, instead of a direct evaluation we choose to treat the coefficients of the *nonlinear* terms, in this case, as free parameters (see also the discussion in Sec. IX).

Since the experimental system is dissipative we add to the amplitude equations (7.2) small phenomenological damping factors. By "small" we mean smaller than $O(\Omega_b-\Omega_a)$ (see also the discussion in Sec. IX).

As a first step we wish to eliminate the trivial, fast time dependence that results from the response at half the driving frequency. To this end we introduce slowly varying amplitudes $a(\tau)$ and $b(\tau)$ defined by

$$\alpha_a(t)=a(\tau)e^{it/2},\quad \alpha_b(t)=b(\tau)e^{it/2}\ , \tag{8.1}$$

where $\tau=\epsilon t$ and ϵ is a small parameter of $O(\Omega_b-\Omega_a)$. When we insert Eqs. (8.1) into Eqs. (7.2) we find

$$\frac{da}{d\tau}=(-L_a+i\phi_a)a+i\Gamma_1\bar{a}+i\Gamma_2|a|^2a+i\Gamma_3|b|^2a+i\Gamma_4\bar{a}b^2\ , \tag{8.2a}$$

$$\frac{db}{d\tau}=(-L_b+i\phi_b)b+i\Delta_1\bar{b}+i\Delta_2|b|^2b+i\Delta_3|a|^2b+i\Delta_4\bar{b}a^2\ , \tag{8.2b}$$

where

$$\Gamma_i=\gamma_i/\epsilon,\quad \Delta_i=\delta_i/\epsilon\ , \tag{8.3}$$

$$\phi_{a,b}=(\Omega_{a,b}-\tfrac{1}{2})/\epsilon\ , \tag{8.4}$$

and L_a,L_b are phenomenological damping constants.

Equations (8.2) can be integrated numerically to explore the phase diagram. The values of the parameters used are displayed in Table I. We discuss the part of the phase diagram that pertains to the immediate vicinity of the criti-

TABLE I. Parameters used to reproduce the phase diagram.

$\omega_a=49.4490\ \text{sec}^{-1}$	$\gamma_2=-5.0\times10^{-3}$
$\omega_b=50.2265\ \text{sec}^{-1}$	$\delta_2=6.5\times10^{-3}$
$\chi_a=1.9249$	$\gamma_3=\delta_3=8.5\times10^{-2}$
$\chi_b=1.9684$	$\gamma_4=\delta_4=0$
$L_a=L_b=5\times10^{-4}/\epsilon$	

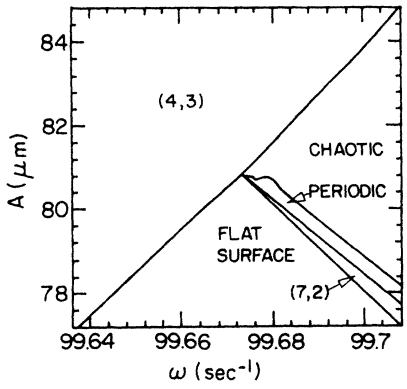

FIG. 7. The theoretical phase diagram in the immediate vicinity of the critical point. A is $2h\,|\,\Lambda\,|$.

cal point (which, strictly speaking, is also the range of validity of our theory). The theoretical phase diagram is shown in Fig. 7. The main characteristics of Fig. 1 are reproduced: (i) the asymmetry between the modes, i.e., the fact that the (4,3) mode damps the (7,2) mode whereas the (7,2) mode pumps the (4,3) mode, (ii) the existence of a region with slow periodic competition between the modes, and (iii) the existence of a chaotic competition. Notice also that the boundaries between these regions converge close to the critical point, as seen experimentally. We note, however, that the chaotic region contains periodic windows as well as long chaotic transients. We also note that a more careful search reveals very small chaotic regions in the "periodic" regime, close to the "boundary" with the chaotic regime. The slight disagreement with the frequency range between Figs. 1 and 7 is due to the inexact boundary conditions used in the theory. The variance in values of A can be easily fixed by adjusting the parameters of Table I. We did not attempt to obtain a "best" fit.

In Figs. 8, 9, 10, and 11 we show typical behaviors which are encountered when the phase diagram is traversed along the $\omega=99.68$ sec^{-1} line. Below

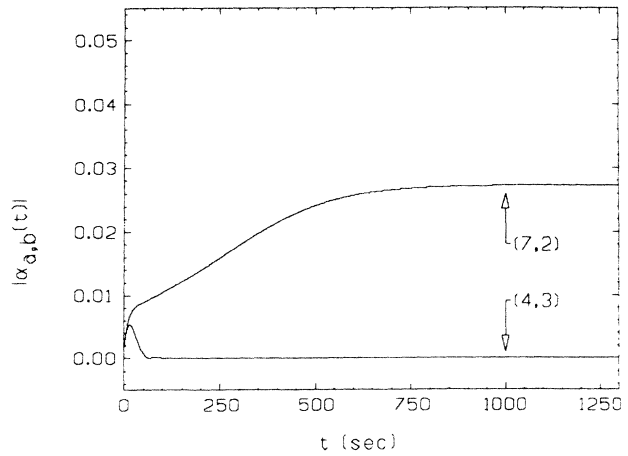

FIG. 8. Time signals for $|\alpha_a|$ and $|\alpha_b|$ at $A=80.16$ μm, $\omega=99.68$ sec^{-1} [(7,2) single mode domain].

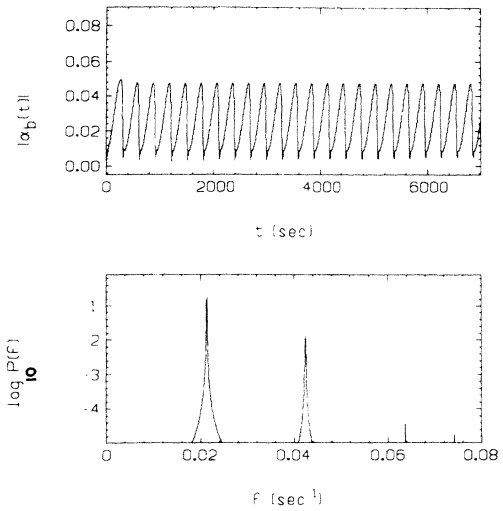

FIG. 9. The signal and power spectrum for $|\alpha_b|$ at $A=80.4$ μm, $\omega=99.68$ sec^{-1} (periodic mode competition domain).

$A\equiv 2h\,|\,\Lambda\,|=80.08$ m the quiescent state prevails. At $a=80.16$ μm (Fig. 8) the seven-fold mode prevails. The magnitude of its amplitude $|\alpha_b(t)|=|b(\tau)|$ grows to a value of about 0.027 and remains stationary at this value. The amplitude of the four-fold mode decays to zero. At $A=80.4$ μm (Fig. 9) slow periodic mode competition takes place. $|\alpha_b(t)|$ [as well as $|\alpha_a(t)|$] oscillates with a single frequency $f\simeq 0.021$ sec^{-1} (and its harmonics). At $A=81.0$ μm (Fig. 10) the competition becomes chaotic. $|\alpha_b(t)|$ [as well as $|\alpha_a(t)|$] has a broad-band power spectrum. Finally, at $A=82.0$ μm (Fig. 11) the four-fold

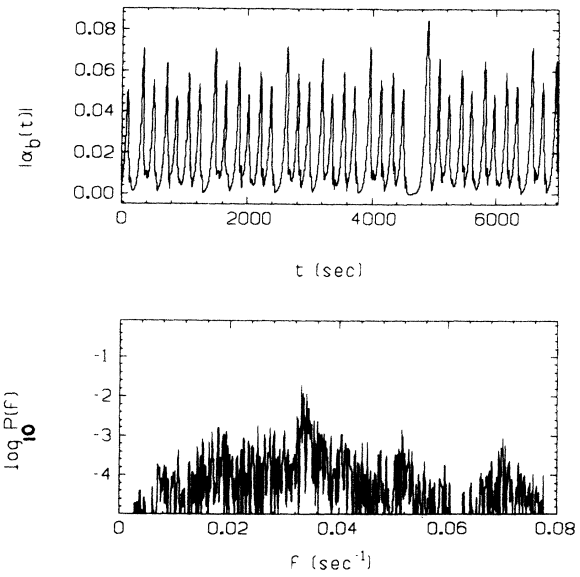

FIG. 10. Time signal and power spectrum for $|\alpha_b|$ at $A=81.0$ μm, $\omega=99.68$ sec^{-1} (chaotic mode competition domain).

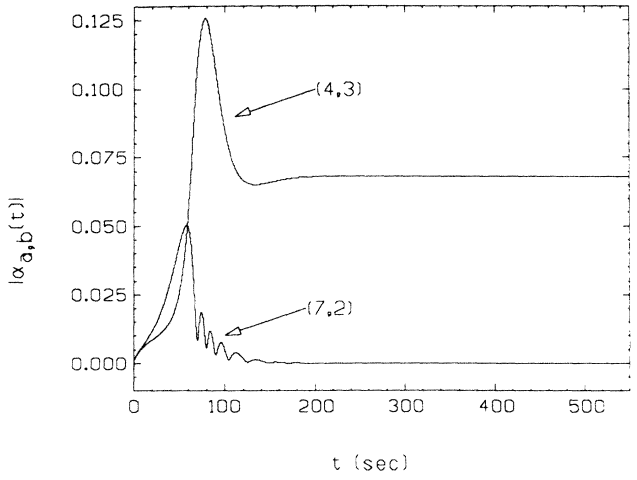

FIG. 11. Time signals for $|\alpha_a|$ and $|\alpha_b|$ at $A=82.0$ μm, $\omega=99.68$ sec^{-1} [(4,3) single mode domain].

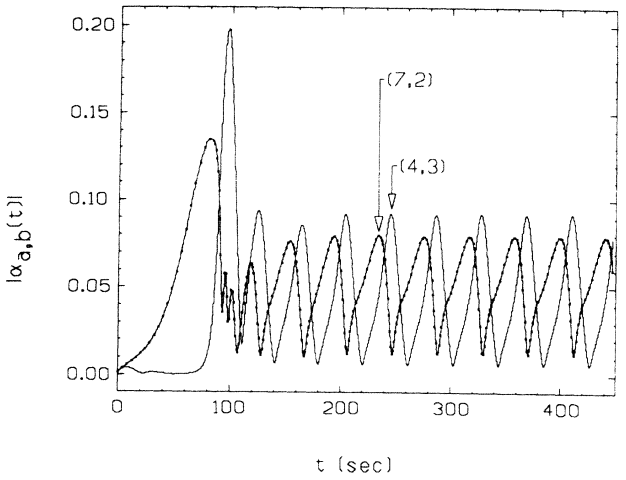

FIG. 13. Time signals for $|\alpha_a|$ and $|\alpha_b|$ at $A=79.066$ μm, $\omega=99.71$ sec^{-1} (periodic window in the chaotic domain).

mode prevails: initially both modes grow but eventually the four-fold mode damps the seven-fold mode and $|\alpha_a(t)|$ becomes stationary ($\simeq 0.068$).

The slow periodic competition is further illustrated in Figs. 12 and 13. Figure 12 corresponds to a point in the periodic regime, while Fig. 13 pertains to a point inside a periodic window in the chaotic regime. The seven-fold mode seems to grow first and then to pump the four-fold mode.

To validate what seemed to be a chaotic motion we have also calculated the maximal Lyapunov exponent. A positive value typically of $O(0.01)$ has been found in the chaotic regime.

IX. SUMMARY AND DISCUSSION

In this paper we have shown that it is possible to obtain, theoretically, low-dimensional chaos from a set of hydrodynamic PDE's in a system of experimental interest. Starting with the hydrodynamic equations (3.14) we derived a set of four nonlinear amplitude equations (7.2) including the coefficients (7.3) (with the exception of the damping factors which were introduced phenomenologically). An expansion (7.4) for the solution to the hydrodynamic equations in terms of the amplitudes and spatial-vector functions was also derived. For the experiment under investigation we were able to rationalize essentially all the major experimental findings: the appearance of regular and chaotic mode competitions, the existence of an asymmetry between the (4,3) and (7,2) modes, the qualitative structure of the phase diagram in the close vicinity of the critical point and the appearance of the stable modes in the solution to the hydrodynamic equations.

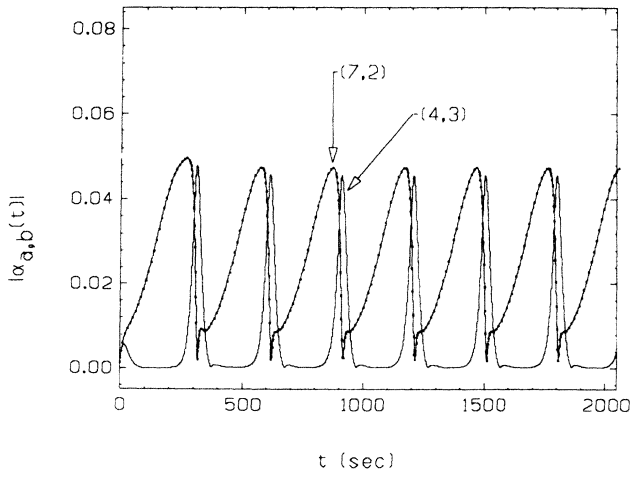

FIG. 12. Time signals for $|\alpha_a|$ and $|\alpha_b|$ at $A=80.4$ μm, $\omega=99.68$ sec^{-1} (periodic mode competition domain).

As noted before the energy dissipation in this system has been taken into account phenomenologically. The neglect of dissipation in the hydrodynamic equations appeared to us unavoidable in order to make the problem tractable. We note in this context that the dissipation of energy is mainly due to friction at the vessel walls[26] and to viscous dissipation in the air layer above the free surface (notice that the kinematic viscosity of air is much larger than that of water).[19] Without dissipation, however, the center-manifold theory would not be applicable, nor would the comparison with the experimental results be possible (no strange attractor, for example, would exist). We therefore had to introduce phenomenological damping factors. These factors are small and thus do not affect the normal-form analysis. We could therefore introduce them at the end of the derivation. We note that along with the damping factors we should also have introduced small real parts to the coefficients of the nonlinear terms in Eqs. (8.2). These, however, did not appear necessary to reproduce the phase diagram.

We might expect that the breaking of the continuous angular symmetry would be accompanied by the appearance of a slow rotational degree of freedom. Such rota-

tional motion, however, has not been observed in the experiment. We therefore ignored this degree of freedom in our analysis and adopted basis functions whose angular parts are either sine or cosine terms with constant phases. This and the boundary condition $\partial\zeta/\partial n=0$ led us to the functions $f_{l,m}$ given by Eq. (4.3). As already pointed out in Sec. VIII these basis functions become problematic when we come to evaluate the coefficients γ_i and δ_i. The difficulties we presented there can be avoided by a slight modification of the experiment, i.e., by using a rectangular cell and a fluid which wets the walls more efficiently. For such an experiment we can employ the analytic expressions (7.17) for the nonlinear terms and obtain, *theoretically,* numerical estimates for γ_i and δ_i.

ACKNOWLEDGMENTS

This work has been supported in part by the Minerva Foundation, Munich, Germany. We benefited from very useful discussions with Professor Ed Spiegel and Professor Jerry Gollub. We thank Jerry Gollub for sharing with us his experimental results prior to publication.

APPENDIX A: EVALUATION OF THE Z DEPENDENCE OF THE VELOCITY POTENTIAL

To derive Eq. (4.5) we first insert the expansion $\phi(x,y,z,t)=\sum_n \phi_n(t,z)f_n(x,y)$ into the Laplace equation $\nabla^2\phi=0$ and use the eigenvalue equation $\nabla_\perp^2 f_n=-h^2k_n^2 f_n$ to obtain

$$\frac{\partial^2\phi_n}{\partial z^2}=h^2k_n^2\phi_n \ . \tag{A1}$$

We now solve Eq. (A1) with the boundary condition

$$\frac{\partial\phi}{\partial z}=0 \quad \text{at } z=1 \ . \tag{3.12b'}$$

The general solution of Eq. (A1) can be written as

$$\phi_n(t,z)=a_n(t)e^{hk_nz}+b_n(t)e^{-hk_nz} \ . \tag{A2}$$

Adopting the notation $\phi_n(t)\equiv\phi_n(t,z=0)$ we find

$$\phi_n(t)=a_n(t)+b_n(t) \ . \tag{A3}$$

Inserting Eq. (A2) into the boundary condition (3.12b') we find

$$b_n(t)=a_n(t)e^{2hk_l} \ . \tag{A4}$$

Solving Eqs. (A3) and (A4) for $a_n(t)$ and $b_n(t)$ and plugging these amplitudes in Eq. (A2) we arrive at the desired result.

APPENDIX B: THE TRANSFORMATION $Z_n(t)^{-1}$

Consider the system

$$\dot U_n=K_n(t)U_n+G(u), \quad K_n(t+2\pi)=K_n(t) \ . \tag{B1}$$

Let W_n be the fundamental matrix of the linearized problem $\dot U_n=K_n(t)U_n$. Then W_n can be written as

$$W_n=Z_n(t)e^{L_nt}, \quad Z_n(t+2\pi)=Z_n(t) \ , \tag{B2}$$

where L_n is time independent. By definition W_n satisfies the linear equation

$$\dot W_n=K_n(t)W_n \ . \tag{B3}$$

We want to show that the transformed amplitudes

$$\tilde U_n=[Z_n(t)]^{-1}U_n \tag{B4}$$

satisfy the equation

$$\dot{\tilde U}_n=L_n\tilde U_n+\tilde G(\tilde u,t), \quad \tilde G(u,t+2\pi)=\tilde G(u,t) \ . \tag{B5}$$

Taking the time derivative of $\tilde U_n$, using the identity $\dot Z_n^{-1}=Z_n^{-1}\dot Z_nZ_n^{-1}$ and Eqs. (B1) and (B4) we find

$$\dot{\tilde U}_n=[Z_n(t)]^{-1}[K_n(t)Z_n(t)-\dot Z_n(t)]\tilde U_n + [Z_n(t)]^{-1}G(u) \ . \tag{B6}$$

Taking now the time derivative of Eq. (B2) and combining the result with Eq. (B3) we find

$$L_n=[Z_n(t)]^{-1}[K_n(t)Z_n(t)-\dot Z_n(t)] \ . \tag{B7}$$

Inserting Eq. (B7) into Eq. (B6) we obtain the desired result (B5) where

$$\tilde G(\tilde u,t)=[Z_n(t)]^{-1}G(u) \ . \tag{B8}$$

APPENDIX C: EVALUATION OF $I^{(k)}$

According to Eqs. (6.19), (6.21), and (6.22), $I^{(k)}$ is given by

$$I^{(k)}=(\alpha_c+\bar\alpha_c)\begin{bmatrix}0&0\\1&0\end{bmatrix}V^{(k-1)} - \sum_{\substack{k_1,k_2>1\\k_1+k_2=k+1}} G^{(k_1)}\cdot\partial_\alpha V^{(k_2)}+\sum_{\substack{k_1,k_2\\k_1+k_2=k}} N[V^{(k_1)}V^{(k_2)}] + \sum_{\substack{k_1,k_2,k_3\\k_1+k_2+k_3=k}} N[V^{(k_1)}V^{(k_2)}V^{(k_3)}] \ , \tag{C1}$$

where

$$N_1[V^{(k_1)}V^{(k_2)}]=-\nabla_\perp V_2^{(k_1)}\cdot\nabla_\perp V_1^{(k_2)}-(\nabla_\perp^2V_2^{(k_1)})V_1^{(k_2)} \ , \tag{C2a}$$

$$N_2[V^{(k_1)}V^{(k_2)}]=-\tfrac12\nabla_\perp V_2^{(k_1)}\cdot\nabla_\perp V_2^{(k_2)}-\tfrac12\chi V_2^{(k_1)}V_2^{(k_2)} \ , \tag{C2b}$$

$$N_1[V^{(k_1)}V^{(k_2)}V^{(k_3)}]=\tfrac12V_1^{(k_1)}V_1^{(k_2)}\nabla_\perp^2\chi V_2^{(k_3)} + V_1^{(k_1)}\nabla_\perp V_1^{(k_2)}\cdot\nabla_\perp\chi V_2^{(k_3)} \ , \tag{C2c}$$

$$N_2[V^{(k_1)}V^{(k_2)}V^{(k_3)}]=V_1^{(k_1)}\nabla_\perp V_2^{(k_2)}\cdot\nabla_\perp(\chi V_2^{(k_3)}) - V_1^{(k_1)}\nabla_\perp^2V_2^{(k_2)}\chi V_2^{(k_3)} \ . \tag{C2d}$$

The expansion (6.37) for $V^{(k)}$ can be written as

$$V^{(k)}=\sum_{i,j} v_{j:i}^{(k)} F_{j:i} \ , \tag{C3}$$

where

$$v_{j:i}^{(k)}=\sum_{L} P_{j:i}^{L} e^{L} \ . \tag{C4}$$

In terms of the multinomials $v_{j:i}^{(k)}$ the terms appearing in Eq. (C1) read

$$(\alpha_c+\bar{\alpha}_c)\begin{bmatrix}0 & 0\\ 1 & 0\end{bmatrix} V^{(k-1)}=\frac{1}{\sqrt{2}}\sum_j f_j \begin{bmatrix}0\\ i(\alpha_c+\bar{\alpha}_c)[v_{j:1}^{(k)}-v_{j:2}^{(k)}]\end{bmatrix} , \tag{C5}$$

$$G^{(k_1)}\cdot\partial_\alpha V^{(k_2)}=\frac{1}{\sqrt{2}}\sum_j \sum_{n=a,\bar{a},b,\bar{b}} f_j G_n^{(k_1)} \begin{bmatrix} i\partial_{\alpha_n}[v_{j:1}^{(k_2)}-v_{j:2}^{(k_2)}]\\ \dfrac{\Omega_j}{\chi_j}\partial_{\alpha_n}[v_{j:1}^{(k_2)}+v_{j:2}^{(k_2)}]\end{bmatrix} , \tag{C6}$$

$$N_1[V^{(k_1)}V^{(k_2)}]=-\tfrac{1}{2}\sum_{j,m}\frac{i\Omega_j}{\chi_j}(\nabla_\perp f_j\cdot\nabla_\perp f_m-k^2k_j^2f_jf_n)[v_{j:1}^{(k_1)}+v_{j:2}^{(k_1)}][v_{m:1}^{(k_2)}-v_{m:2}^{(k_2)}] , \tag{C7a}$$

$$N_2[V^{(k_1)}V^{(k_2)}]=-\tfrac{1}{4}\sum_{j,m}\frac{\Omega_j\Omega_m}{\chi_j\chi_m}(\nabla_\perp f_j\cdot\nabla_\perp f_m+\chi_j\chi_m f_jf_m)[v_{j:1}^{(k_1)}+v_{j:2}^{(k_1)}][v_{m:1}^{(k_2)}+v_{m:2}^{(k_2)}] , \tag{C7b}$$

$$N_1[V^{(k_1)}V^{(k_2)}V^{(k_3)}]=\frac{1}{4\sqrt{2}}\sum_{j,m,n}\Omega_n(k^2k_n^2f_jf_mf_n-2f_j\nabla_\perp f_m\cdot\nabla_\perp f_n)[v_{j:1}^{(k_1)}-v_{j:2}^{(k_1)}][v_{m:1}^{(k_2)}-v_{m:2}^{(k_2)}][v_{n:1}^{(k_3)}+v_{n:2}^{(k_3)}] , \tag{C7c}$$

$$N_2[V^{(k_1)}V^{(k_2)}V^{(k_3)}]=\frac{1}{2\sqrt{2}}\sum_{j,m,n}\frac{i\Omega_m\Omega_n}{\chi_n}(k^2k_m^2f_jf_mf_n+f_j\nabla_\perp f_m\cdot\nabla_\perp f_n)[v_{j:1}^{(k_1)}-v_{j:2}^{(k_1)}][v_{m:1}^{(k_2)}+v_{m:2}^{(k_2)}][v_{n:1}^{(k_3)}+v_{n:2}^{(k_3)}] . \tag{C7d}$$

[1]D. Ruelle and F. Takens, Chem. Math. Phys. **20**, 167 (1971).

[2]M. J. Feigenbaum, J. Stat. Phys. **19**, 25 (1978); **21**, 669 (1979).

[3]A. Libchaber and J. Maurer, in *Nonlinear Phenomena at Phase Transitions and Instabilities,* edited by T. Riste (Plenum, New York, 1981); See also, *Hydrodynamic Instabilities and the Transition to Turbulence,* edited by H. L. Swinney and J. P. Gollub (Springer, Berlin, 1981).

[4]I. Procaccia, Phys. Scr. **59**, 40 (1985), and references therein.

[5]Examples are E. Knobloch and J. Guckenheimer, Phys. Rev. A **27**, 408 (1983); H. R. Brand, P. C. Hohenberg, and V. Steinberg, Phys. Rev. A **30**, 2548 (1984); also Refs. 6 and 7.

[6]P. Coullet and E. A. Spiegel, SIAM J. Appl. Math. **43**, 776 (1983).

[7]A. Arneodo, P. H. Coullet, and E. A. Spiegel, Geophys. Astrophys. Fluid Dynamics **31**, 1 (1985).

[8]H. R. Brand, P. C. Hohenberg, and V. Steinberg, Phys. Rev. A **27**, 408 (1983).

[9]Such a theory has been achieved in the context of mechanical systems, see P. Holmes and J. Marsden, Arch. Natl. Mech. Anal. **76**, 135 (1981); F. C. Moon and P. J. Holmes, J. Sound Vib. **65**, 275 (1979).

[10]M. Faraday, Philos. Trans. R. Soc. London **121**, 299 (1831).

[11]L. Matthiessen, Ann. Phys. (Leipzig) **134**, 107 (1868); **141**, 375 (1870).

[12]Lord Rayleigh, Philos. Mag. **16**, 50 (1883).

[13]Lord Rayleigh, Philos. Mag. **15**, 235 (1883).

[14]T. B. Benjamin and F. Ursell, Proc. R. Soc. London, Ser. A **225**, 505 (1954).

[15]R. Keolian, L. A. Turkevich, S. J. Putterman, and I. Rudnick, Phys. Rev. Lett. **47**, 1133 (1981).

[16]J. P. Gollub and C. W. Meyer, Physica **6D**, 337 (1983).

[17]S. Ciliberto and J. P. Gollub, Phys. Rev. Lett. **52**, 922 (1984); J. Fluid Mech. (to be published).

[18]E. Meron and I. Procaccia, in *Complex Systems,* edited by H. Haken (Springer, Berlin, 1986); E. Meron and I. Procaccia, Phys. Rev. Lett. **56**, 1323 (1986); a related study is that of J. W. Miles, in J. Fluid Mech. **146**, 285 (1984). The analysis in this study is based on a Lagrangian formulation which leads to a Hamiltonian system for the critical degrees of freedom. It does not apply, however, to the strongly nonlinear motions which have been observed in the experiment.

[19]L. D. Landau and E. M. Lifshitz, *Fluid Mechanics* (Pergamon, New York, 1959).

[20]See, for example, D. W. Jordan and P. Smith, *Nonlinear Ordinary Differential Equations* (Oxford University Press, London, 1977).

[21]M. Abramowitz and I. A. Stegun, *Handbook of Mathematical Functions* (Dover, New York, 1972).

[22]S. H. Davis and S. Rosenblat, Stud. Appl. Math. **57**, 59 (1977).

[23]We were informed by S. Ciliberto that when the surface in the experiment becomes polluted (this influences the contact angles) the mode (11,1) could be seen.

[24]J. Carr, *Applications of Centre Manifold Theory* (Springer-Verlag, New York, 1981).

[25]V. I. Arnol'd, *Geometrical Methods in the Theory of Ordinary Differential Equations* (Springer-Verlag, New York, 1983).

[26]J. W. Miles, Proc. R. Soc. London, Ser. A **297**, 459 (1967).